ARTICLES

Stream Incision, Tectonics, Uplift, and Evolution of Topography of the Sierra Nevada, California

John Wakabayashi and Thomas L. Sawyer[1]

1329 Sheridan Lane, Hayward, California 94544, U.S.A.
(e-mail: wako@tdl.com)

ABSTRACT

Stream incision, faulting, thermochronologic, and geobarometric data suggest that Sierra Nevada topography is a consequence of two periods of uplift. Stream incision of up to 1 km has occurred since ~5 Ma. Maximum Eocene-Miocene incision was 150 m. Uplift of the Sierra Nevada, westward tilting, stream incision, and east-down normal and dextral faulting along the present eastern escarpment of the range began at ~5 Ma. Estimates of Late Cenozoic crestal rock uplift for different areas in the Sierra Nevada range from 1440 to 2150 m. Low summit erosion rates suggest that the rock uplift approximates the surface uplift of crestal summits. Tertiary stream gradients were lower than modern ones, suggesting that the bottoms of the canyons have been uplifted in the Late Cenozoic and that the mean elevation of the Sierra Nevada has increased. The elevation of pre-Cenozoic basement rocks above the base of Tertiary paleochannels ranges from <200 m in the northern part of the range to >1000 m in the south, and shows that significant relief predates Late Cenozoic incision. Elevations at ~5 Ma (before Late Cenozoic uplift) may have been <900 m in the northern Sierra and >2500 m in the southern Sierra. Minimal Eocene-Miocene stream incision suggests that paleorelief and paleoelevations are relics of pre-Eocene uplift. Reduction of elevation and relief following pre-Eocene uplift may have coincided with eclogitic recrystallization of the mafic root of Sierran batholith. This eclogitic keel may have foundered in the Late Cenozoic, triggering uplift.

Introduction

The 600-km-long Sierra Nevada is the most prominent mountain range in California. The Sierra Nevada and the Central Valley are part of the Sierra Nevada microplate, an element of the broad Pacific-North American plate boundary (Argus and Gordon 1991) (fig. 1). The dextral movement of the Sierra Nevada microplate relative to stable North America is ~10–14 mm/yr, directed subparallel to the plate boundary (Argus and Gordon 1991; Dixon et al. 2000). Internal deformation of the microplate is minor compared with deformation along its boundaries. The microplate is bounded on the west by an active fold and thrust belt that marks the eastern margin of the Coast Range province (e.g., Wentworth and Zoback 1989) and on the east by a prominent east-facing escarpment that marks the Sierra

Nevada frontal fault system ("frontal fault system"), a zone of normal, normal dextral, and dextral faulting (e.g., Clark et al. 1984; Beanland and Clark 1995) (figs. 1, 2). For purposes of discussion, the frontal fault system is considered the westernmost element of the dextral Walker Lane Belt that separates the Sierra Nevada microplate from the Basin and Range province.

Before becoming part of the transform plate margin, arc magmatism occurred in the Sierra Nevada. Mesozoic arc activity included the emplacement of the Sierra Nevada batholith and ended at ~85 Ma (Saleeby and Sharp 1980; Stern et al. 1981; Chen and Moore 1982). Cenozoic volcanism, some of which was associated with the development of a magmatic arc, blanketed much of the northern and central Sierra from about 35 to 5 Ma (e.g., Christiansen and Yeats 1992). The southernmost active volcano of the Cascades arc is Mount Lassen (fig. 1), and earlier Late Cenozoic volcanic arc activity
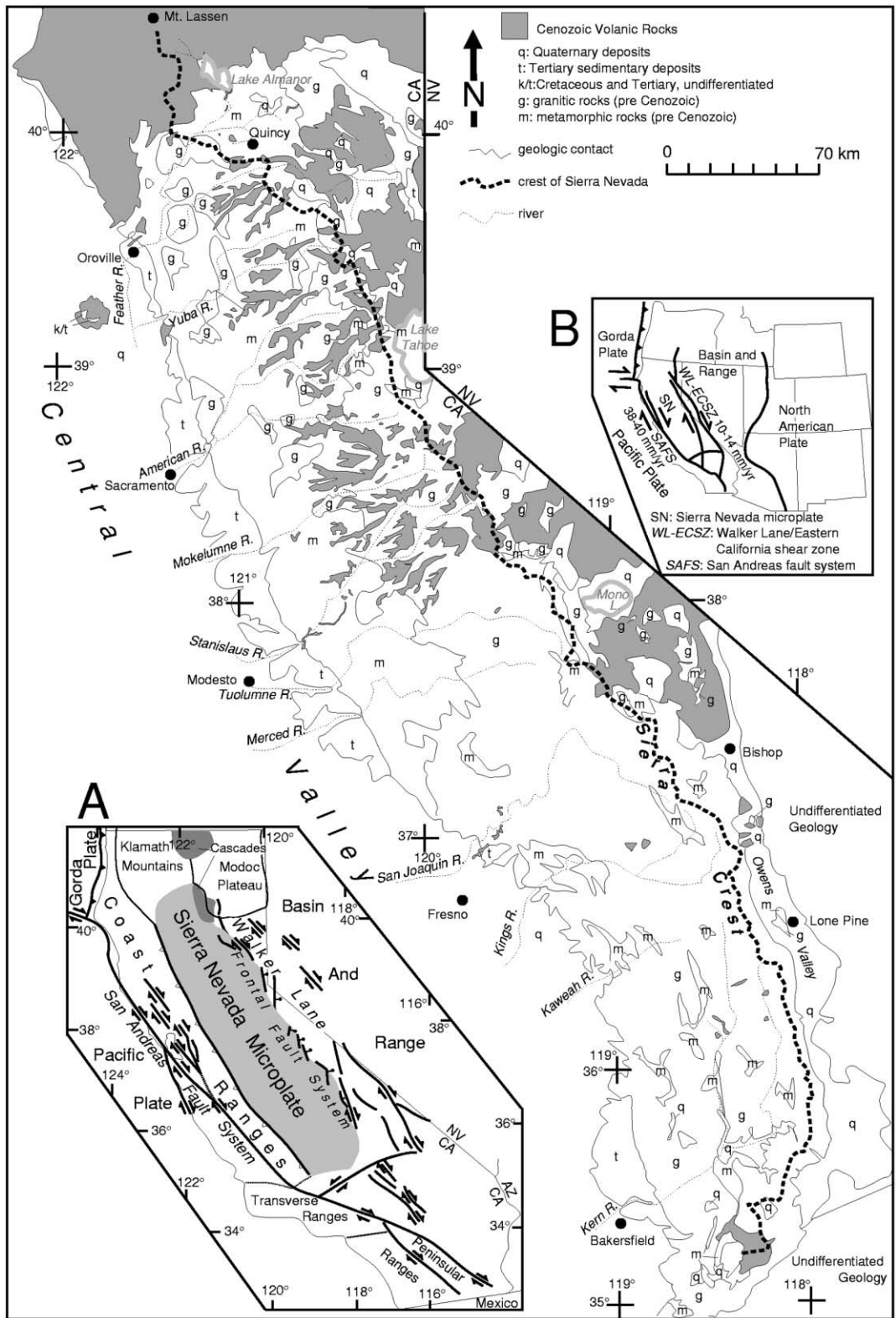
Figure 1. Generalized geologic map of the Sierra Nevada, showing Quaternary alluvium, Cenozoic volcanic rocks (*shaded*), granitic rocks, and metamorphic rocks. Adapted from Wakabayashi and Sawyer (2000).
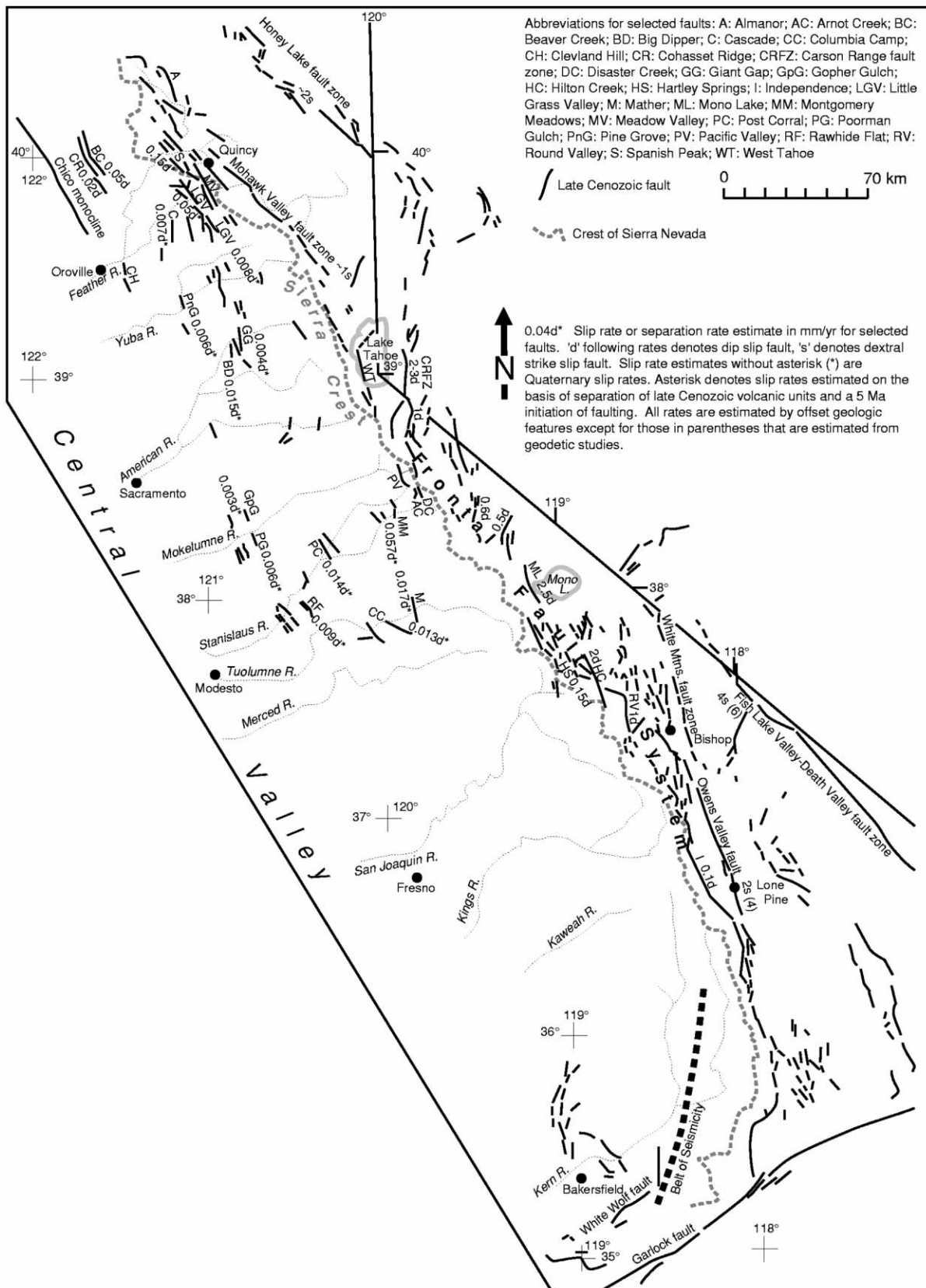
Figure 2. Generalized Late Cenozoic fault map of the Sierra Nevada. Adapted from Wakabayashi and Sawyer (2000)

extended as far south as the Stanislaus River drainage (within what is now the Sierra Nevada) before shutting off as the Mendocino triple junction migrated northward and the convergent plate margin was replaced by a transform one (e.g., Atwater and Stock 1998). Cenozoic volcanic deposits cover basement (pre-Cenozoic metamorphic and plutonic rocks) in the northern and central Sierra (fig. 1) and provide constraints on Late Cenozoic deformation of the Sierra Nevada (faults shown in fig. 2).

The Sierra Nevada slopes gently westward and abruptly eastward from its crest (fig. 3); this asymmetry reflects westward tilting and vertical deformation along the frontal fault system. In the northern part of the range, the westward slope has a relatively constant gradient, whereas in the southern part of the range, it slopes gently west of the crest and steepens in the western foothills (fig. 3). Crestal elevations vary from 2100 to 2700 m in the northern part of the range to 4000 to 4400 m in the central to southern part of the range, with the highest elevations in the headwaters of the Kings and Kern Rivers and maximum elevations decreasing to the south. The height of the eastern escarpment varies from about 1000 m in the northernmost part of the range to nearly 3300 m at Lone Pine (fig. 3).

Early researchers concluded that most of the elevation of the range was a consequence of Late Cenozoic uplift and tilting associated with major faulting along the eastern margin of the range (e.g., Whitney 1880; Ransome 1898; Lindgren 1911). Christensen (1966), Huber (1981, 1990), and Unruh (1991) refined estimates of the timing and magnitude of uplift. Paleobotanical data suggest that paleoelevations in the range were lower, implying significant Late Cenozoic uplift (e.g., Axelrod and Ting 1960; Axelrod 1962, 1997). In contrast, thermochronologic studies have concluded that mean elevation and relief of the Sierra Nevada has been decreasing progressively since the Late Cretaceous (House et al. 1998).

In this article, we present and summarize data on stream incision, tilting, faulting, and sediment accumulation and evaluate data on geochronology, thermochronology, and geobarometry. These data will be used to show (1) the neotectonic evolution of the Sierra Nevada, including the evolution of the eastern boundary of the Sierran microplate; (2) the relationship of faulting, tilting, and stream incision to uplift; and (3) the contribution of different stages of uplift to the present topography of the range. We will show that the topography of the mountain range is a consequence of two major uplift events: a Late Cenozoic one and one that occurred at least 50 m.yr. earlier in a different tectonic setting. This study demonstrates the complexity of tectonic events that can contribute to the topographic evolution of a major mountain range.

Cenozoic Stratigraphy of the Sierra Nevada

Estimates of Cenozoic stream incision and deformation are best constrained where Cenozoic deposits are present in the Sierra Nevada (fig. 1). Widespread Cenozoic deposits are limited to the area north of the Tuolumne River (fig. 1). The oldest of the Cenozoic cover strata are Eocene gold-bearing gravels, commonly referred to as the "auriferous gravels," and their fine-grained equivalents along the eastern margin of the Central Valley, the Ione Formation (e.g., Bateman and Wahrhaftig 1966). Overlying the Eocene deposits are 20–34-Ma rhyolite tuffs, including the Valley Springs and Delleker Formations (Wagner et al. 1981; Saucedo and Wagner 1992). These rhyolites are overlain by 4–14-Ma andesites, andesitic mudflows, and associated volcanic sedimentary rocks (Bartow 1979; Wagner et al. 1981; Saucedo and Wagner 1992); the term "Mehrten Formation" will be used generically to describe these rocks, following the broad definition of Curtis (1954). The Mehrten Formation blanketed the northern and central Sierra, covering all but a few scattered basement highs (Durrell 1966; Slemmons 1966). The age of the upper Mehrten is important because the initiation of significant incision and faulting was synchronous with, or shortly followed, the deposition of these units. In the Mokelumne River drainage, the upper Mehrten is interpreted to be ~4 Ma, on the basis of K/Ar ages of two dacitic plugs that intrude the Mehrten, one of which is overlain by uppermost Mehrten strata (Bartow 1979). Andesitic deposits in the headwaters of the North Fork American River have K/Ar ages of 3.3–5.4 Ma (Harwood 1986 data in Saucedo and Wagner 1992); some of these deposits may be proximal equivalents of the upper Mehrten of the northern Sierra. North of the Yuba River, the youngest K/Ar age from Mehrten rocks is 6.8 Ma (Saucedo and Wagner 1992), but there are too few ages in this region to reliably constrain age of the youngest Mehrten. For the purposes of discussion, an age of ~5 Ma for the upper Mehrten is used in this article for discussion of rangewide processes.

Northward younging of the youngest Late Cenozoic volcanic rocks in the Sierra Nevada may be expected because of the northward migration of the Mendocino triple junction and associated shutoff of subduction and arc volcanism, but there is too much scatter in the age data to confirm such a pattern. Volcanic rocks younger than 4 Ma are lo-
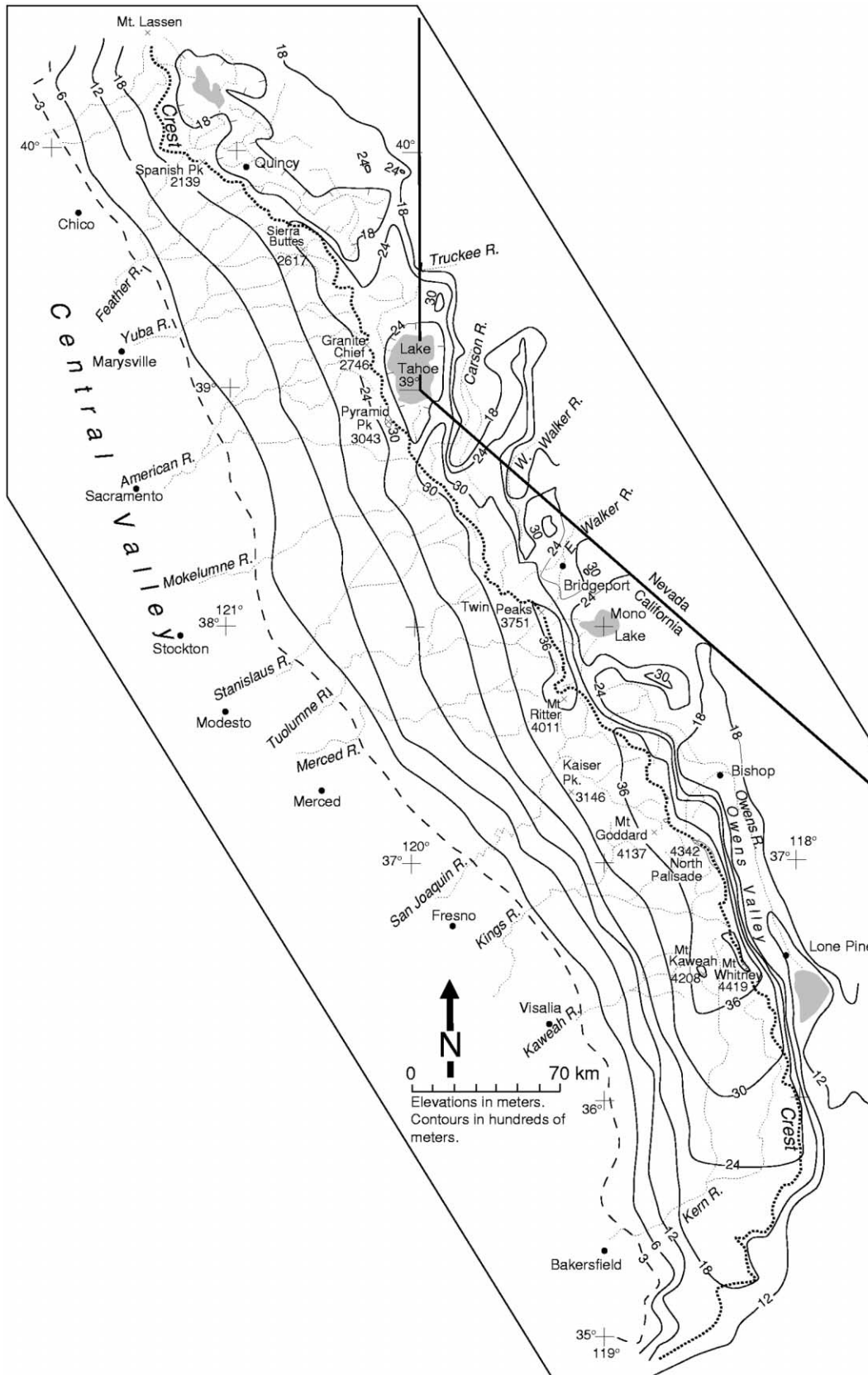
Figure 3. Generalized topography of the Sierra Nevada. Similar to the methodology of Christensen (1966); the contouring smooths over stream-cut canyons but shows major fault escarpments.

cally present and are most common in the Donner Summit region (i.e., the crestal area northwest of Lake Tahoe in fig. 1) and the northernmost Sierra (north of the Feather River in fig. 1).

The Eocene gravels, Valley Springs Formation, and Mehrten Formation are most extensively preserved north of the Tuolumne River within the Sierra Nevada; minor accumulations of these deposits are found along the eastern margin of the Central Valley as far south as the Kings River (e.g., Bartow 1985, 1990). Widely scattered outcrops of Miocene to Late Quaternary volcanic rocks occur south of the Tuolumne River (Moore and Dodge 1980). These volcanic rocks represent local eruptive events associated with extensional tectonics rather than the Cenozoic volcanic arc and, before erosion, constituted a much smaller volume than Mehrten Formation rocks to the north (Ducea and Saleeby 1998).

Stream Incision Rates

Significant Late Cenozoic stream incision in the northern and central Sierra is demonstrated by the occurrence of Late Cenozoic deposits capping divides and ridges hundreds of meters above canyon bottoms incised into basement. Long-term Late Cenozoic incision rates can be estimated by measuring the elevation difference between the present channels and the tops of Late Cenozoic deposits capping the interfluves and dividing the elevation difference by the age of the youngest of the deposits. We refer to such incision as "total incision" (fig. 4; table 1). Most of the uppermost Late Cenozoic deposits are mudflows of the Mehrten Formation and related rocks. These deposits blanketed nearly the entire Sierra north of the Tuolumne River drainage so that any streams in this area had to downcut through them. Thus, the observed incision apparently occurred in the last ~5 Ma. Some incision would likely follow deposition of these volcanic rocks whether or not tectonic tilting occurred because the emplacement of large amounts of volcanic deposits in drainages may have changed local base levels. For example, the Mehrten Formation locally occupies channels up to 250 m deep cut into older Cenozoic volcanic rocks in the headwaters of the Stanislaus River, but the maximum channeling of Mehrten Formation into the Eocene gravels in most areas is about 60 m, including areas where Valley Springs Formation is lacking beneath the Mehrten (Lindgren 1911; Yeend 1974). These relations suggest that incision of Mehrten into older Cenozoic volcanic rocks may be at least partly a consequence of local base level change caused by
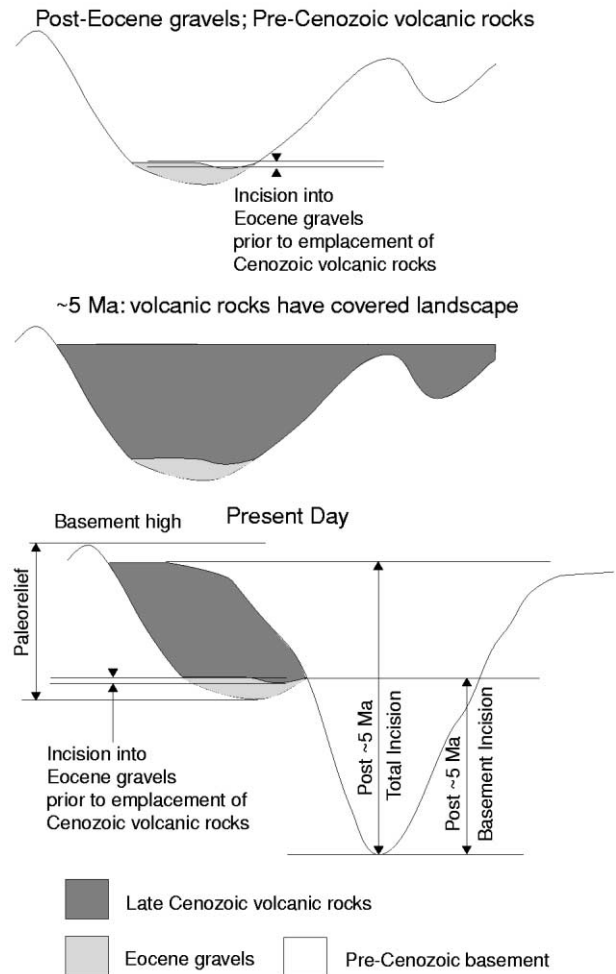
Figure 4. Diagram depicting the evolution of the cross section of a typical Sierra Nevada canyon, showing how the terms "paleorelief," "total incision," and "basement incision" are defined in this article. At many localities, Late Cenozoic volcanic rocks directly overlie basement rather than Eocene gravels.

volcanic deposition. Accordingly, we have also estimated incision rates on the basis of the elevation difference between the bottom of Late Cenozoic volcanic deposits and the present canyon bottom. We refer to this incision as "basement incision" (fig. 4; table 1). Such rates are minima because time required for the stream to cut through the volcanic rocks is not considered. In the San Joaquin River drainage, incision was estimated with respect to the reconstructed position of the 10-Ma ancestral channel, as well as to the 3.4–3.9-Ma volcanic rocks that were erupted into the canyon (Huber 1981).

Post-Mehrten incision in the northern and central Sierra Nevada ranges up to 1340 m of total incision and 1190 m of basement incision (table 1;

Table 1. Deepest Cenozoic Incision and Corresponding Rates

	Minimum incision (m)[a]	Incision rate[b]	Time range
North Fork Feather River	1340 (1190)	.27 (.24)	5 Ma to present
Middle Fork Feather River	950 (830)	.19 (.17)	5 Ma to present
North Yuba River	915 (640)	.18 (.13)	5 Ma to present
North Fork American River	1130 (700)	.23 (.14)	5 Ma to present
North Fork Mokelumne River	1150 (980)	.23 (.20)	5 Ma to present
Stanislaus River	1075 (710)	.22 (.14)	5 Ma to present
Tuolumne River	(890)	(.18)	5 Ma to present
San Joaquin River	(580)	(.089)	10 to 3.5 Ma
	(390)	(.11)	3.5 Ma to present
Post-Eocene to Miocene Incision:[c]			
Yuba River drainage	≤60	<.003	...
American River drainage	150	<.007	...

[a] Incision below volcanic rocks in parentheses.
[b] Except where noted, minimum basement incision rate in parentheses.
[c] Averaged over 20 m.yr., the minimum age difference between the youngest Eocene gravels and oldest Mehrten Formation.

fig. 5). For the major drainages, Late Cenozoic basement incision rates associated with the deepest parts of the canyons range from 0.10 to 0.24 mm/yr, and total incision rates range from 0.10 to 0.27 mm/yr (table 1). Rates estimated for the San Joaquin River are somewhat lower than those estimated for other drainages, although the amount of incision is similar. Post-3.5-Ma incision rates there are essentially the same as post-10-Ma rates (Huber 1981; table 1), suggesting that incision began much earlier in this drainage than in other major drainages to the north. It is possible that the ages of the 3.4–3.9-Ma basalts (Dalrymple 1964), upon which the post-3.5-Ma incision rates are based, are too old; some K/Ar dates of Cenozoic volcanic rocks, particularly basaltic rocks, have been shown to be inaccurate, on the basis of subsequent Ar/Ar step heating dates (e.g., Sharp et al. 1996). Initiation of Late Cenozoic incision of the San Joaquin River at approximately the same time as in drainages to the north (~5 Ma) is consistent with observation that tilts and ages of Late Cenozoic strata along the eastern margin of the Central Valley are similar from the Feather River to the Kings River (Unruh 1991).

In the North Fork Feather River, upstream of its confluence with the East Branch North Fork, a succession of volcanic flows, with ages of 2.8, 2.1, 1.1, and 0.6 Ma, was deposited into the ancestral canyon (Wakabayashi and Sawyer 2000). These flows are now preserved as terrace-like remnants on the walls of the canyon, and river gravels are present locally along the base of the remnants. The volcanic remnants record a cyclic history of lava flowing down the ancestral North Fork canyon, followed by river incision through the flow, another flood of lava down the canyon, and renewed inci-

sion. The oldest flows are preserved as the highest remnants above the present stream bottom, whereas the youngest flows are preserved as the lowest remnants. This relationship has been confirmed by Ar/Ar dating of the volcanic units (Wakabayashi et al. 1994). On the basis of the elevation of volcanic rocks in the North Fork Feather River canyon, it appears that incision rates from 1.1 to 0.6 Ma and from 1.1 Ma to present are higher than incision rates from 2.1 to 1.1 Ma or 2.8 to 1.1 Ma by a factor of 2–3 or more (table 2) (Wakabayashi and Sawyer 2000).

A minimum age for the regional onset of Late Cenozoic incision in the Sierra Nevada is ~3.5–4 Ma, on the basis of the occurrence of basalts within the inner canyons of Sierran drainages (Dalrymple 1964; Huber 1981) and the age of Pliocene strata that unconformably overlies more steeply tilted Miocene-Pliocene strata along the eastern margin of the Central Valley (Unruh 1991). The maximum age of the onset of the Late Cenozoic incision is the age of the upper Mehrten Formation (~5 Ma). The incision data for the North Fork Feather River show temporal variations in incision rate in the North Fork Feather River since 2.8 Ma, with higher Quaternary rates than the Late Cenozoic average.

Eocene to Miocene incision rates were much lower than Pliocene incision rates. The maximum incision of Miocene volcanic rocks into or through Eocene strata is <60 m in most areas (Lindgren 1911; Yeend 1974), but is locally as much as 150 m (Bateman and Wahrhaftig 1966). The minimum age difference between the youngest Eocene gravels and oldest Mehrten Formation is ~20 Ma. Averaging 150 m of incision over 20 Ma yields 0.007
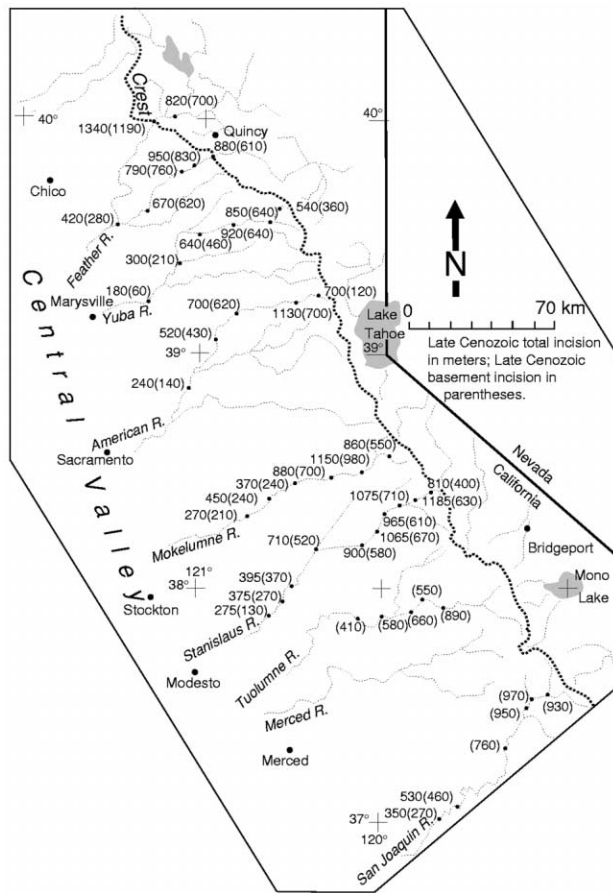
Figure 5. Late Cenozoic stream incision of the northern and central Sierra Nevada.

mm/yr as a maximum Eocene to Miocene incision rate.

Paleorelief: Relief That Predates Late Cenozoic Deposits

Minimum topographic relief that existed at the time of the deposition of Cenozoic deposits may be estimated by comparing the elevation of basement topographic highs relative to the elevation of the local base of Cenozoic strata (fig. 4) (Bateman and Wahrhaftig 1966). The elevation difference is a minimum estimate of relief that predated Late Cenozoic stream incision (referred to as paleorelief) because some erosional lowering of topographic highs had occurred during the Late Cenozoic. The amount of lowering of these topographic highs in the Late Cenozoic is probably small; erosion rates measured for bedrock summit flats of the Sierra Nevada and other western North American mountain ranges are low, ranging from 2 to 15 m/Ma

(0.002–0.015 mm/yr) over the last 35–236 ka (Small et al. 1997) (Sierra Nevada values are 0.002–0.005 mm/yr but are derived from only three samples). Evaluation of paleorelief is possible only north of the San Joaquin River because Cenozoic deposits are too scattered to the south.

Paleorelief in the Sierra Nevada increases from north to south, with a significant increase south of the Stanislaus River drainage (fig. 6). Most of the region north of the American River has paleorelief of <200 m. Paleorelief is >1500 m in parts of the San Joaquin drainage (fig. 6). The southward increase in paleorelief coincides with the southward increase in elevation in the range (figs. 3, 6). In addition, the steeper western slope along the southern Sierra corresponds to an abrupt eastward increase from 100 to >600 m in paleorelief along the San Joaquin drainage (Huber 1981). The distribution of paleorelief suggests that the major along strike differences in topographic expression of the range are largely a consequence of greater paleorelief in the southern compared with the northern part of the range. This is consistent with the hypothesis of Wahrhaftig (1965), who argued that the west-facing topographic escarpments of the south-central and southern Sierra were erosional in origin and not Late Cenozoic fault scarps. Apparent down-west faulting is associated with west-facing topographic steps in the Tuolumne River drainage (Wakabayashi and Sawyer 2000), although the vertical separation of this faulting is much less than half of the height of any associated step.

Late Cenozoic Faulting and Neotectonics of the Sierra Nevada

Late Cenozoic Faulting along the Frontal Fault System. The frontal fault system varies along strike. South of Bishop, the eastern boundary of the Sierran block is marked by a major dextral fault, the Owens Valley fault, and by a continuous escarpment formed by east-down normal faults (fig. 2). North of Bishop, where much of the dextral slip diverges eastward, the range front is composed of a series of left-stepping en echelon escarpments that reflect normal or oblique faulting. From Bishop to Bridgeport, each of these en echelon escarpments does not extend far from the eastern margin of the range, whereas north of Bridgeport, individual escarpments continue northward as major faults bounding mountain ranges that extend into Nevada, far from the Sierra proper (fig. 3). This geometry persists as far north as the Tahoe Basin. North of the Tahoe Basin, the dextral Mohawk Valley fault zone marks the eastern boundary of the Sierra. In the

Table 2. Incision Rate, North Fork Feather River, Lake Almanor to Confluence with East Branch North Fork Feather River

Fault block or reach of river	Total incision rate (mm/yr) with time interval[a]
Ohio Creek to Salmon Creek	.57–.73 Ma to present: .21–.26 (.096–.12); 1.11–1.20 Ma to present: .22–.24 (.16–0.17); 1.11–1.20 Ma to .57–.73 Ma: .31–.52 (.18–.31)
Davis Creek to Meeker Bar	.57–.73 Ma to present: .30–.38 (.10–.13); 1.11–1.20 Ma to present: .29–.31 (.24–.25); 1.11–1.20 Ma to .57–.73 Ma: .43–.71 (.33–.54); 2.05 Ma to 1.11–1.20 Ma: .13–.15 (.052–.058)
Butt Creek to Crablouse Ravine	.57–.73 Ma to present: .37–.48 (.15–.19); 1.11–1.20 Ma to .57–.73 Ma: .43–.72 (.31–.51); 1.11–1.20 Ma to present: .32–.34 (.25–.27)
Crablouse Ravine to Mosquito Creek	.57–.73 Ma to present: .28–.36 (.14–.18); 1.11–1.20 Ma to .57–.73 Ma: .32–.54 (.21–.35)
Mosquito Creek to Queen Lily	.57–.73 Ma to present: .29–.37 (.067–.086); 1.11–1.20 Ma to .57–.73 Ma: .39–.64 (.31–.51)
Waller Creek fault to East Branch confluence	.57–.73 Ma to present: .23–.29 (.12–.15); 1.11–1.20 Ma to .57–.73 Ma: 034–.57 (.24–.40); 2.81 Ma to 1.11–1.20 Ma: .14 (.082–.086); 2.81 Ma to present: .17 (.13)

[a] Parentheses denote basement incision rate.

vicinity of Quincy, the frontal fault system broadens so that faulting is distributed on many strands in a zone 30–40 km wide (fig. 2) (Wakabayashi and Sawyer 2000).

In the Feather River drainage, the vertical separation of the ~5-Ma Mehrten Formation and 16-Ma Lovejoy Basalt across faults of the frontal fault system ranges from about 600 to 1000 m (Wakabayashi and Sawyer 2000). The east-down vertical separation of Late Cenozoic rocks across the faults bounding the west side of the Lake Tahoe basin may be >1500 m, on the basis of the position of Late Cenozoic volcanic rocks west of the lake and the minimum thickness of Quaternary sediments that may overlie similar volcanic rocks beneath the lake (Hyne et al. 1972). In the headwaters of the Stanislaus River drainage, the vertical separation of the ~9-Ma Eureka Valley tuff is about 1100 m (Slemmons 1966; Noble et al. 1974). At the headwaters of the San Joaquin River, a 2.2–3.6-Ma volcanic unit is vertically separated by ~980 m across the frontal faults (Bailey 1989). The aggregate vertical separation of these volcanic rocks between crestal exposures and their buried correlatives in the Long Valley Caldera may be as much as 2.1 km (Bailey 1989), but much of this separation may be a consequence of caldera collapse instead of frontal faulting.

Gravity data have been interpreted as indicating 2.1 km of downdropping and filling of Owens Valley with sediments in the Cenozoic (Pakiser et al. 1964). Bachman (1978) interpreted 1.1-km down-dropping in the last 2.3 Ma from the same data. Vertical separation across the frontal fault system is equal to the infill depth plus the escarpment height generated by Late Cenozoic faulting (which is difficult to estimate because of the scarcity of Late Cenozoic deposits near the crest). Phillips (2000) correlated basaltic scoria deposits on the Sierran crest west of Bishop with a volcanic center in Owens Valley, suggesting 2500 m of post-3.5-Ma east-down vertical separation across the frontal fault system.

Timing of Late Cenozoic Vertical Separation along the Frontal Fault System: Westward Encroachment during the Late Cenozoic.   Most of the Late Cenozoic volcanic rocks of the central and northern Sierra Nevada had sources east of the frontal fault system (e.g., Durrell 1966; Slemmons 1966), suggesting that Frontal faulting did not begin until after the eruption of these deposits; the flows could not have flowed uphill across the fault scarps. Some of the major river drainages of the mountain range such as the San Joaquin (Matthes 1930; Huber 1981), Stanislaus, and Yuba River (Lindgren 1911) drainages, have been beheaded by movement along the frontal faults. The relationship of Frontal faulting to beheaded drainages and the distribution of volcanic rocks suggests that the frontal fault system and Walker Lane Belt have encroached westward in the Late Cenozoic.

In the Feather River area, down-east separation of the 16-Ma Lovejoy Basalt and overlying Mehrten Formation across frontal faults is the same, indi-
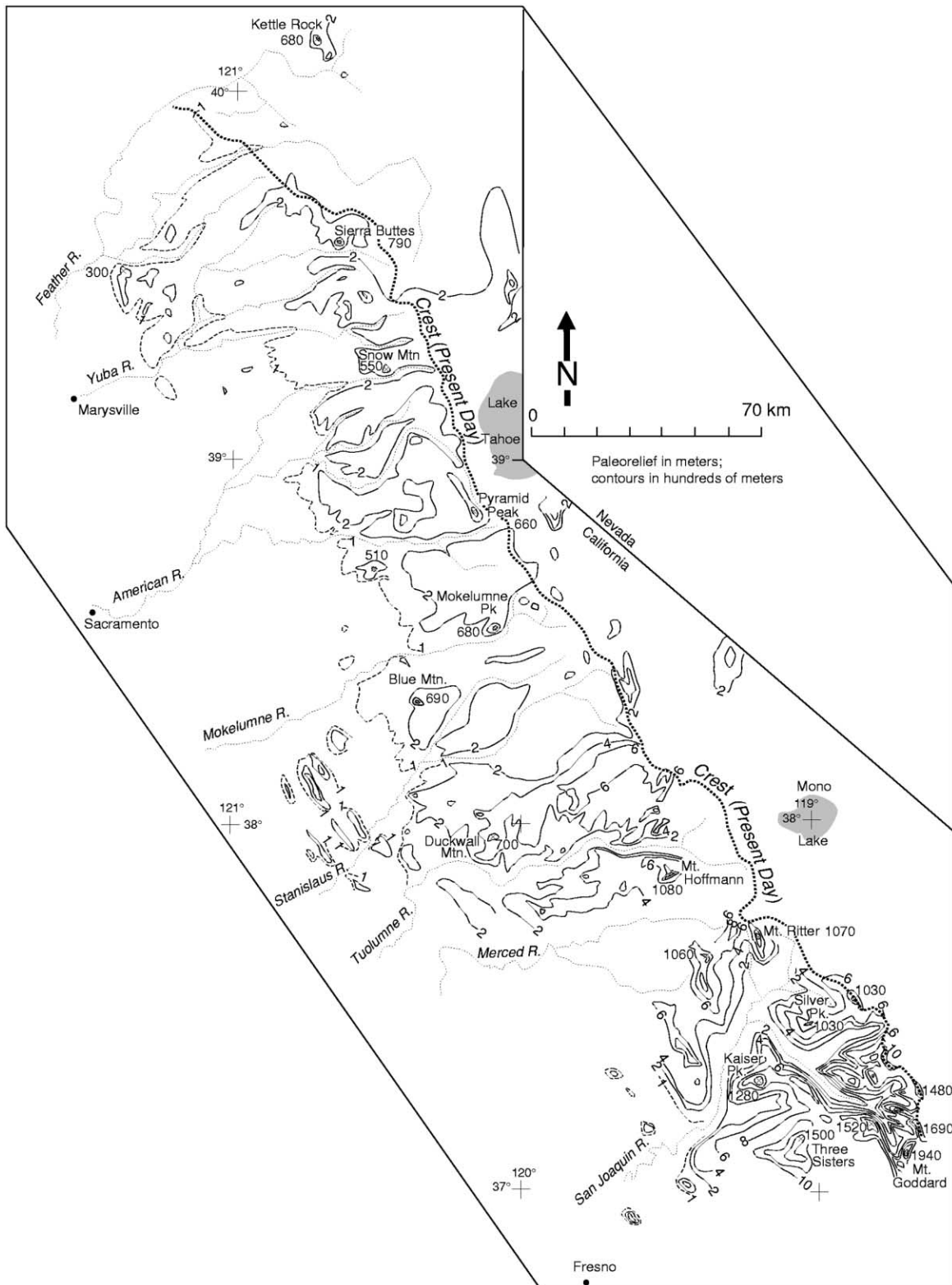
Figure 6. Paleorelief of the northern and central Sierra Nevada recorded by the difference in elevation between basement highs and the local base of Cenozoic deposits. In the San Joaquin River drainage, the paleorelief is estimated with respect to the reconstructed position of the 10-Ma paleochannel of Huber (1981). This map shows paleorelief preserved today rather than a reconstruction of inferred paleorelief at 5 Ma; this is why modern streams correspond to areas of low paleorelief on the map.

cating that faulting did not commence until after Mehrten deposition (Wakabayashi and Sawyer 2000). Accordingly, frontal faulting in the Feather River area probably began some time after ~5 Ma. Before the establishment of the present frontal fault system, the northern Sierran block may have extended eastward to the Honey Lake fault zone, east of the crest of the Diamond Mountains (fig. 2). Movement on the Honey Lake fault zone postdates the 10-Ma Thompson Peak Basalt, which has a source east of the escarpment and is faulted across it (Roberts 1985). Movement on some of the most significant faults of the frontal fault system crossing the North Fork Feather River canyon probably did not begin until after 600 ka (Wakabayashi and Sawyer 2000). Thus, the western margin of the Walker Lane Belt appears to have stepped 50 km westward, from the Honey Lake area to the present eastern escarpment of the northern Sierra Nevada, within the last 5 Ma, and has encroached into the northernmost part of the range since the mid to Late Quaternary.

Westward encroachment of the western Walker Lane Belt margin may have occurred along most of the tectonic boundary. The western edge of the central Walker Lane Belt from 38° to 39°N progressively stepped 100 km westward from 15 to 7 Ma, on the basis of detailed structural, stratigraphic, and geochronologic studies (Dilles and Gans 1995). East of the Lake Tahoe area, major east-down faulting began after 10 Ma, on the basis of interpretation of syntectonic sediments in the Verdi basin (Trexler et al. 1999), and at 7 Ma in the Gardnerville basin, on the basis of syntectonic basal sediments (Muntean et al. 1999). The data from these basins are consistent with the westward progression of faulting noted by Dilles and Gans (1995). Slemmons et al. (1979) also suggested westward encroachment of the Walker Lane into the Sierran block in the Late Cenozoic, with somewhat broader age constraints.

At the headwaters of the Middle Fork San Joaquin River, vertical movement along the frontal fault system could not have begun until after ~3 Ma; otherwise, a 2.2–3.6-Ma volcanic flow would have been blocked by fault scarps (Bailey 1989). Before 3 Ma, the frontal fault system must have been east of the headwaters of the ancestral San Joaquin River, which is at least 40 km east of the present position of the fault system (Huber 1981).

Bachman (1978) suggested that Sierran escarpment in the Owens Valley area did not form until 2.3–3.4 Ma. Bachman's (1978) data and observations constrain timing of the uplift of the White Mountains (the range east of Owens Valley), but do not directly constrain movement on the frontal fault system. However, the correlation of volcanic deposits by Phillips (2000) suggests that frontal faulting in the Bishop area is younger than 3.5 Ma. South of Owens Valley, lacustrine deposits are overlaid by volcanic rocks that have yielded dates as old as 6 Ma, indicating that a basin existed in that area before 6 Ma (Bacon et al. 1979).

In the southern Sierra, a belt of seismicity (fig. 2), characterized by east-down normal fault focal mechanisms, has been interpreted as an incipient westward jump of the frontal fault system (Jones and Dollar 1986). The topography across this zone is consistent with major faulting, but there are no Late Cenozoic deposits to verify that the topography reflects Late Cenozoic vertical separation (Wakabayashi and Sawyer 2000).

Late Cenozoic Internal Deformation of the Sierra Nevada: How Rigid is the Rigid Block? Late Cenozoic internal deformation of the Sierra Nevada, recorded by faulting and local tilting of Late Cenozoic deposits, is minor compared with faulting along the frontal fault system (e.g., Lindgren 1911; Bateman and Wahrhaftig 1966; Christensen 1966). The deformation of Late Cenozoic units that span the Sierra indicates that internal deformation is distributed evenly across the range (see more detailed discussions in Wakabayashi and Sawyer 2000) (figs. 1, 2). Internal deformation is most significant in the area directly west of the crest; this deformation appears to be related to en echelon east-down frontal faults that cross the crest (Wakabayashi and Sawyer 2000) (fig. 2). Projection of the tilts of the Lovejoy Basalt and Table Mountain Latite from the western margin of the Sierra Nevada to the crest appears to overestimate the actual crestal elevations of these strata at the crest by 315–365 m compared with their actual outcrop elevations (details are in the appendix, which is available from *The Journal of Geology*'s Data Depository free of charge upon request). This minor departure from rigid block tilting is primarily a consequence of significant east-down faulting directly west of the crest. Similar deformation near the crest may be expected in much of the Sierra north of the Kings River headwaters.

Uplift of the Sierra Nevada

Sierra Nevada uplift has been estimated on the basis of analyses of tilted strata (e.g., Lindgren 1911; Grant et al. 1977; Huber 1981; Unruh 1991) and paleobotany (e.g., Axelrod 1962). Such uplift estimates are subject to alternative interpretations. Progressively steeper tilts of progressively older

Late Cenozoic strata on the western margin of the range may be interpreted to be a consequence of progressive tilting and Late Cenozoic crestal rock uplift of the range (Grant et al. 1977; Unruh 1991), or alternatively, to reflect original slopes on a range that has been progressively lowered (implicit in the model of decreasing relief and elevation of House et al. 1998). Moreover, tilt and uplift of ridge tops may have occurred even if there was little change in mean elevation (Small and Anderson 1995). Paleobotanical studies are also subject to contrasting interpretations (e.g., Axelrod 1997; Wolfe et al. 1997). In the following sections, we show that Late Cenozoic mean surface uplift, and probably pre-Eocene rock and surface uplift of the Sierra Nevada, occurred; we also present estimates for the amount of uplift and its variation along the strike of the range.

Relationship of Stream Incision, Uplift, Topography, and Thermochronology: Did Late Cenozoic Uplift Occur? Late Cenozoic basement incision is up to 1190 m along parts of major river drainages of the Sierra. The magnitude of Late Cenozoic incision may be different for areas south of the limit of Late Cenozoic cover strata. However, the similarity of tilt for Late Cenozoic strata of the same age as far south as the Kings River (Unruh 1991), as well as the comparable incision in areas of contrasting topographic expression described above, suggests similar magnitudes of Late Cenozoic incision at least as far south as the Kings River. The bottoms of the most deeply incised canyons represent the deepest exposure of rocks that were buried before Late Cenozoic erosion in the Sierra. The maximum Late Cenozoic basement incision of ~1 km is probably too small to have been recorded by either (U-Th)/He apatite dating (45°–85°C range of partial retention of He in apatite [Wolf et al. 1998]) or apatite fission-track dating (60°–125°C is the partial annealing zone for apatite fission tracks [e.g., Dumitru 1990]). Accordingly, (U-Th)/He ages from the Sierra record cooling and exhumation (mean ages of 45–85 Ma) (House et al. 1997, 1998) immediately following emplacement of the youngest Sierran plutons that occurred at ~85 Ma (e.g., Stern et al. 1981; Chen and Moore 1982). Sphene fission track data show cooling below ~270°C by 73 Ma for plutons that crystallized at 100–110 Ma, and apatite fission-track data show cooling below 95°C at about 67 Ma for plutons that crystallized at 86–110 Ma (Dumitru 1990). Reduced lengths of apatite fission tracks have been interpreted as evidence for 2–3 km of Late Cenozoic exhumation (Dumitru 1990). However, this estimated exhumation exceeds the ~1-km maximum erosion on the basis of Late Ce-

nozoic stream incision, and the samples showing the most significant track length reduction were taken from near ridge tops where erosion is very much less than the maximum incision (Small et al. 1997).

House et al. (1998) suggested that thermochronologic data indicate that the peak elevation of the Sierra Nevada was attained in the Cretaceous and that elevations and topographic relief have been progressively decreasing since then, with no uplift in the Late Cenozoic. Their conclusions were primarily based on (1) modeling of (U-Th/He) ages that suggest several kilometers of relief during the time of cooling and (2) an elevation model that suggested that Cretaceous mean crestal elevations were higher than the present. If topographic relief has been progressively decreasing, then erosion rates on ridge tops should exceed stream incision rates; but the data of Small et al. (1997) indicate that erosion rates of summit flats range from 0.002 to 0.015 mm/yr, compared with incision rates of 0.1 mm/yr or more. These data indicate that relief in the Sierra Nevada has been increasing recently rather than decreasing (e.g., Small and Anderson 1998). In addition, the House et al. (1998) model of progressively decreasing elevation implies that the progressively steeper westward gradients of progressively older Late Cenozoic strata reflect the original stream gradients, not progressive Late Cenozoic tilting and uplift. If true, stream gradients and stream power, and hence, stream incision rates, would be expected to have progressively decreased since the Cretaceous. Progressively decreasing stream power is inconsistent with stream incision data that indicate low incision rates (<0.007 mm/yr) from the Eocene to Miocene, and rapid incision (≥0.1 mm/yr) in the last 5 Ma. The interpretation of significant relief during the Cretaceous and early Cenozoic is consistent with the existence of paleorelief and does not preclude subsequent Late Cenozoic uplift and increase of relief.

Small and Anderson (1995) suggested that Late Cenozoic increase in peak elevations of the Sierra has been balanced by erosion of canyons, so that there has been negligible change in average elevation of the Sierra in the Late Cenozoic. However many studies have concluded that Tertiary stream gradients were lower than present-day gradients upstream of the hingeline for tilting, on the basis of the broad, alluviated nature of the paleovalleys compared with the narrow, bedrock-floored modern canyons (e.g., Bateman and Wahrhaftig 1966; Christensen 1966; Huber 1981, 1990) (fig. 7). The interpretation of low Tertiary stream gradients is consistent with the low Eocene-Miocene incision
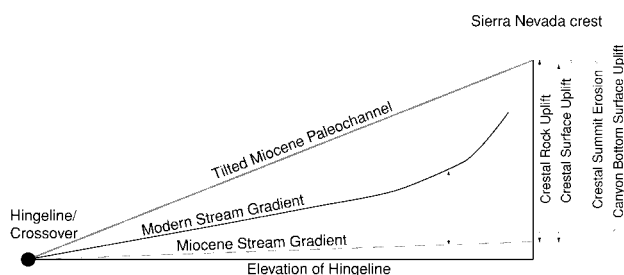
Figure 7. Diagram showing the relationship of tilted Miocene paleochannels, Miocene stream gradients, modern stream gradients, and erosion to surface and rock uplift of the Sierra Nevada.

rates noted above. On the basis of the similarity of Miocene and modern-day flood plain deposits at the hingeline, Huber (1981) and Unruh (1991) concluded that the flood plain environment was similar, implying that hingeline has maintained the same elevation (~100 m above sea level) during the Late Cenozoic. If the hingeline has stayed at the same elevation and modern streams have higher gradients than their Tertiary precursors, then the canyon bottoms must have been uplifted in Late Cenozoic time (fig. 7). Thus, the mean surface elevation of the range must have increased in the Late Cenozoic.

Early Exhumation, Erosion, and Probable Associated Uplift: 100–60 Ma. The first period of exhumation and possible uplift that influenced current Sierran topography may have begun before to shortly after the intrusion of the last major plutons of the Sierra Nevada batholith (~85 Ma) and probably concluded before Eocene (~50 Ma) sedimentary rocks were deposited on the batholithic and metamorphic basement. The granitic rocks have experienced up to 19–23 km of exhumation, and there is a pronounced transverse gradient with about 10 km more exhumation in the western Sierra than in the crestal area (Ague and Brimhall 1988). A north-south gradient in exhumation magnitude is not apparent except for the very southernmost part of the range. Although major exhumation occurred, the amount of associated surface uplift is unknown because no indicators of elevation relative to sea level have been identified.

Additional time constraints for the exhumation event may be provided by the sedimentary record in the Great Valley Group (fig. 8). It is not possible to account for all of the sediment eroded from the Sierra Nevada because part of the western Great Valley basin was uplifted and eroded; some sediment from the Sierra Nevada bypassed or over-

topped the forearc high and was transported to the trench; and depocenters shifted through time (e.g, Ingersoll 1979; Moxon 1988). However, maximum accumulation rates in the Great Valley Group and younger Central Valley deposits may be interpreted to be proportional to rates of erosion of the Sierra for different time periods. Figure 8, derived from the data of Moxon (1988) for Late Cretaceous and Bartow (1985) for Cenozoic deposits, shows high sediment accumulation rates from about 99 to 57 Ma (Cenomanian to Paleocene), probably indicating a corresponding period of high erosion rates in the Sierra Nevada. The low apparent erosion rates after ~57 Ma indicate that significant exhumation had probably ceased by this time. The sediment accumulation rates for the 99–57-Ma period are higher than those for the Late Cenozoic (post-5 Ma) period (fig. 8).

Erosion rates in the Sierra in the 100–57-Ma age range can be estimated by evaluating the crystallization depths and ages of plutons directly overlapped by Eocene deposits. The youngest such plutons are ~100 Ma, on the basis of U/Pb zircon ages (Stern et al. 1981; Chen and Moore 1982) and comparison of K/Ar hornblende ages of Evernden and Kistler (1970) within areas covered by U/Pb zircon ages with regions that lack U/Pb zircon ages. Most plutons at ~100 Ma in the Sierra Nevada crystallized at depths of 11–15 km (Ague and Brimhall 1988). Accordingly, the long-term average exhumation rate between the time of crystallization and overlap by Eocene deposits is ~0.26–0.35 mm/yr, using the base of Eocene (57 Ma) as the end of the exhumation event because of the drastic reduction in sedimentation rates recorded in the Great Valley Group after this time. Because deformation in the Sierra Nevada during this time was likely transpressional or contractional (e.g., Renne et al. 1993; Tobisch et al. 1995; Tikoff and de Saint Blanquat 1997) instead of transtensional or extensional, it is probable that tectonic exhumation was negligible and that exhumation rates for this time were approximately equal to erosion rates. The long-term erosion rates of 0.26–0.35 mm/yr estimated for the 100–57-Ma time period are significantly greater than the Late Cenozoic erosion rates; the 100–57-Ma rates reflect spatially averaged erosion rates, whereas the highest Late Cenozoic erosion rates are associated with maximum stream incision (0.1–0.2 mm/yr). Average Late Cenozoic erosion rates are lower than the maximum incision rates and are an average of the points of maximum erosion and areas that are eroding much more slowly, such as the downstream parts of the drainages and upland surfaces (Small et al. 1997; Riebe et al. 2000). The high
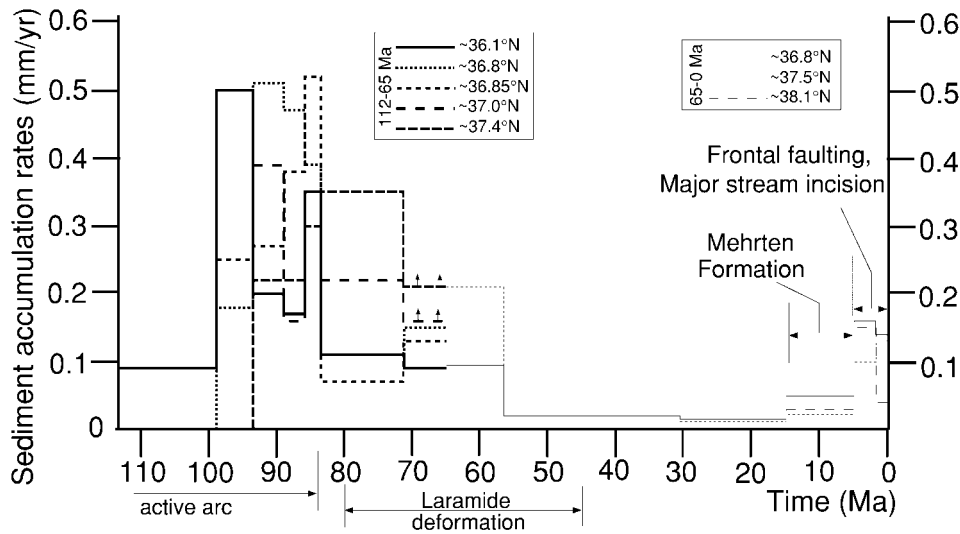
Figure 8. Accumulation rates in the San Joaquin basin. Rates are calculated from unit thicknesses of Moxon (1988) for Cretaceous deposits and of Bartow (1985) for Cenozoic deposits, and time scales of Gradstein et al. (1995) for the Cretaceous and of Berggren et al. (1995) for the Cenozoic. Upward pointing arrows above accumulation rate lines denote minimum rates. The Cretaceous part of the diagram is restricted to the San Joaquin basin, and the Cenozoic part is restricted to the eastern part of the northern San Joaquin basin because sediment sources other than the Sierra may contribute to other parts of the Great Valley basin (the Klamath Mountains for the Cretaceous Sacramento Valley basin and the Tehachapi Mountains and Coast Ranges for the southern and western parts of the Cenozoic San Joaquin basin).

erosion rates for the 100–57-Ma time period suggest that uplift may have been significant during this time period as well, although surface uplift had probably ceased some time before 57 Ma, given that the surface upon which the Eocene deposits were deposited was one of comparatively low relief. Thus, the earlier part of the 100–57-Ma period may have been associated with surface uplift and increase of relief, whereas relief and elevation reduction may have occurred during the latter part of this period.

Minor or Negligible Eocene-Miocene Uplift. Eocene rocks along the eastern margin of the Central Valley are tilted more steeply than the Oligocene and Miocene rocks that overlie them (Huber 1981; Unruh 1991). The difference in tilt has been interpreted as evidence for significant Eocene to Miocene uplift because with a rigid tilt model, Eocene strata projects from the eastern Central Valley to crestal elevations that are 1000 m or more above Miocene strata (Huber 1981). However, Eocene strata lies directly under Miocene and Oligocene strata nearly everywhere where it occurs in the range, including areas near the Sierra crest (e.g., Lindgren 1911; Yeend 1974). Apparently, Eocene strata are tilted more steeply than Miocene and Oligocene strata only along the Central Valley mar-

gin. The occurrence of Eocene beneath Oligocene and Miocene strata in the crestal region suggests that little crestal rock uplift occurred from Eocene to Miocene time. The Mehrten Formation is locally incised up to 150 m into the Eocene gravels (Bateman and Wahrhaftig 1966). This may reflect a low average incision rate between Eocene and Miocene time (<0.007 mm/yr) or negligible Eocene-Oligocene incision followed by moderate incision in the Early to Middle Miocene. The latter alternative is consistent with the conclusions of Huber (1981), who suggested a gradual acceleration of Late Cenozoic uplift and associated incision starting at 25 Ma. In contrast, low sediment accumulation rates in the Central Valley are consistent with little uplift and erosion occurring during Eocene to Miocene time (fig. 8).

Late Cenozoic (Post-Late Miocene) Uplift. Three methods of estimating Late Cenozoic uplift are based on the tilt of Late Cenozoic strata; we describe these methods and their assumptions below (illustrated in fig. 9). All three methods are dependent on the hingeline for tilting maintaining the same elevation throughout the Late Cenozoic; the constant elevation of the hingeline has been shown by Huber (1981) and Unruh (1991). Uplift has been estimated from the tilt of Late Cenozoic strata in

the westernmost Sierra (Huber 1981; Unruh 1991). For this method, the angular difference in tilt between the Late Cenozoic units and the estimated original gradient of the stream (paleogradient) in which the Late Cenozoic units were deposited is projected across the width of the range to obtain an uplift estimate; rigid-block tilting is assumed in

order to project strata eastward from the hingeline. Uplift has also been estimated on the basis of profiles of Late Cenozoic units that span the Sierra (Wakabayashi and Sawyer 2000); such estimates do not depend on a rigid tilt-block model because the elevation of Late Cenozoic strata is known within the interior and at the crest of the range. For range-spanning Late Cenozoic units, estimates of paleogradients are used to estimate the paleoelevation of a marker horizon, and this paleoelevation is subtracted from the present outcrop elevation to estimate uplift. In addition, uplift has been estimated from reaches of paleodrainages with different trends (Lindgren 1911; Huber 1990). For this method, the angular difference between the gradient of axis-perpendicular (presumed to be fully tilted) and axis-parallel (presumed to be untilted) deposits is projected across the width of the range from the hingeline. Uplift estimated with this method is based on rigid block tilting and may be subject to comparatively large uncertainties as a consequence of the relatively short distances that gradients are measured over.

Uplift estimates derived from tilted Late Cenozoic strata are dependent on estimates of paleogradients of the Cenozoic drainages. On the basis of the similarity of channel deposits beneath the ~9-Ma Kennedy Table Mountain trachyte and present-day fluvial deposits on the flood plain of the eastern San Joaquin Valley, Huber (1981) estimated the paleogradient of the western part of the ancestral (~10 Ma) stream drainage as 1 m/km. Channel deposits beneath the Kennedy Table Mountain trachyte are typical of channel deposits of the western reaches of major Miocene Sierra streams. In contrast, the modern river channels upstream of where the Tertiary and modern channels cross in elevation
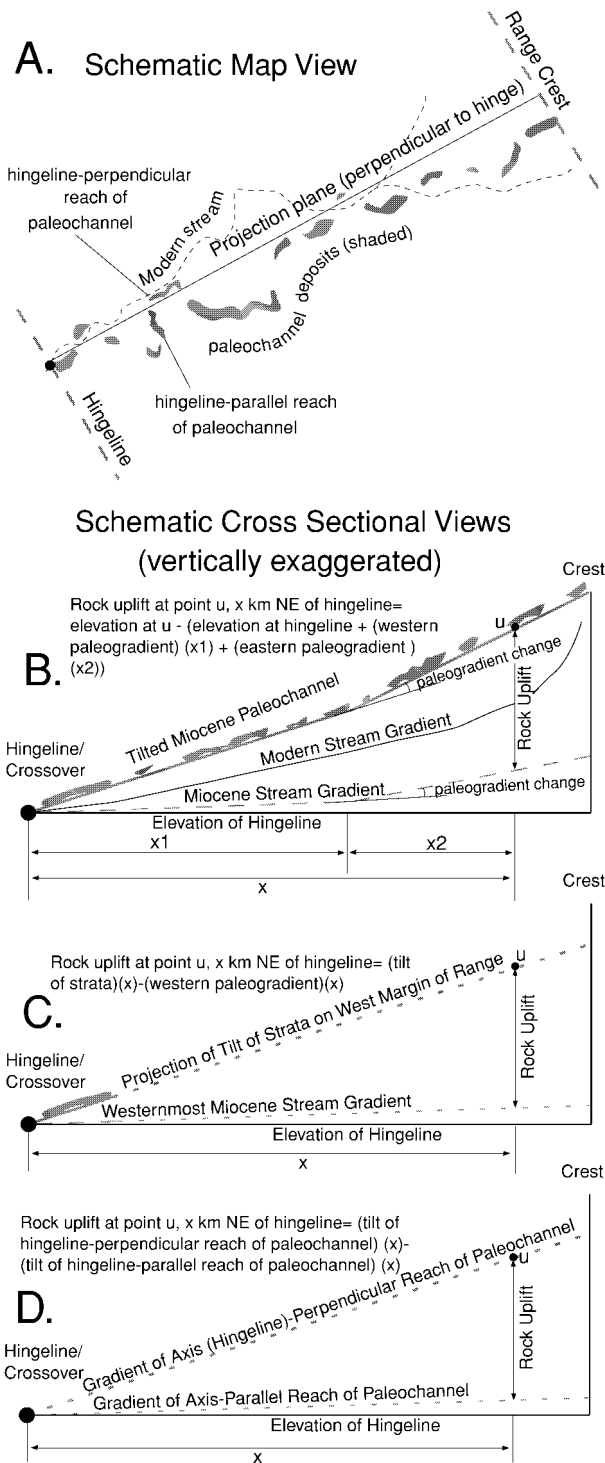
Figure 9. Diagrams showing three methods of estimating Late Cenozoic rock uplift of the Sierra Nevada from tilted Cenozoic strata. *A*, Some map view features of the various methods. *B*, Uplift estimation using Cenozoic deposits that span the range (Wakabayashi and Sawyer 2000). *C*, Uplift estimation based on projecting tilts of strata eastward from the westernmost part of the Sierra (Huber 1981; Unruh 1991). *D*, Uplift estimates based on the different tilts of hingeline-perpendicular (assumed to record full Late Cenozoic tilt) and hingeline-parallel (assumed to be untilted) reaches of paleochannel deposits (Lindgren 1911; Huber 1990). For each method, the formula for estimating uplift is given with the cross section. For these formulae, horizontal distances are in kilometers, the rock uplift is in meters, and the paleogradients and tilts are in meters per kilometer.

(herein termed the "crossover point") are significantly steeper than the paleogradients of the Tertiary streams (Bateman and Wahrhaftig 1966; Christensen 1966; Huber 1981, 1990). Thus, the gradient of the modern streams, measured for several kilometers upstream of the crossover point, can be considered a maximum western paleogradient for Miocene channels. The profiles of range-spanning Late Cenozoic units can be used to estimate points or reaches where paleogradients changed upstream (Huber 1981; Wakabayashi and Sawyer 2000).

Previous and new estimates of Late Cenozoic uplift are summarized in table 3. Below, we will discuss new estimates on the basis of reconstructions of range-spanning Late Cenozoic units. Detailed notes on methodology used in estimating Late Cenozoic Sierran uplift are presented in the appendix. Wakabayashi and Sawyer (2000) estimated 1860 m and 1930 m of uplift on the basis of the reconstructions of the 16-Ma Lovejoy Basalt and the 9-Ma Table Mountain Latite, respectively, and a 1 m/km paleogradient for the westernmost reach of the paleodrainages. We obtained minimum uplift estimates for the Lovejoy Basalt (1710 m) and Table Mountain Latite (1790 m) on the basis of the gradients of the westernmost reaches of the modern streams upstream of the crossover points of the Feather River and Stanislaus Rivers, respectively. On the basis of a westernmost paleogradient of 1 m/km, we have estimated Late Cenozoic uplift of 1690 m for the ancestral Mokelumne River, and 1940 m for the ancestral South Fork American River channel. Our minimum uplift estimates of 1520 m and 1440 m for the ancestral Mokelumne and South Fork American drainages, respectively, are based on western reaches of the modern rivers upstream of the crossover points. The deposits of the ancestral Mokelumne and South Fork American River thalwegs are not as well preserved as the Lovejoy Basalt and Table Mountain Latite. Consequently, uplift estimates for the Mokelumne and South Fork American River are subject to greater uncertainty than those based on reconstructions of the Lovejoy Basalt and Table Mountain Latite.

Estimates of Late Cenozoic uplift fall within a relatively narrow range of 1440–2150 m (table 3). We believe that the best-constrained estimates are those for the Lovejoy Basalt (1710–1860 m), Table Mountain Latite (1790–1930 m), and the ancestral San Joaquin River (2150 m; Huber 1981). Reconstructions of the Lovejoy Basalt and Table Mountain Latite suggest that uplift estimates based on the rigid tilt block model (such as Huber 1981) may be 315–365 m too high as a consequence of east-down deformation directly west of the crest. If similar internal deformation occurs in the San Joaquin drainage then the crestal uplift for that area may be ~1800 m. Thus, our preferred range of Late Cenozoic uplift estimates is 1710–1930 m. Within uncertainty, the amount of Late Cenozoic uplift appears to be similar from the Feather River to the San Joaquin River. This is consistent with the conclusions of Unruh (1991), who suggested that uplift did not vary significantly from the Feather River to the Kings River, on the basis of the constancy

Table 3. Late Cenozoic Crestal Uplift Estimates

Basis of estimate	Width (km)[a]	Uplift (m)
Differential tilt of Late Cenozoic strata, easternmost Central Valley (Unruh 1991)	80, 100	1950, 2440
Reconstruction of Lovejoy Basalt (Wakabayashi and Sawyer 2000; this study)	70	1710–1860
Reconstruction of ancestral South Fork American channel (this study)	100	1440–1940
Paleobotany, Carson Pass (Axelrod 1997)	NA	2500
Reconstruction of ancestral Mokelumne River channel (this study)	95	1520–1690
Reconstruction of Stanislaus Table Mountain Latite and related rocks (Wakabayashi and Sawyer 2000; this study)	90	1790–1930
Reconstruction of ancestral Tuolumne River channel (Huber 1990)	97	>1480
Paleobotany, headwaters of San Joaquin (Axelrod and Ting 1960)	100	2000
As above, adjusted by Huber (1981)	100	1000
Reconstruction of ancestral San Joaquin River base level (Huber 1981)	100	2150

Note.   NA, not applicable.
[a] The distance between the hingeline and the point of highest uplift measured perpendicular to the tilt axis.

of tilts of Late Cenozoic strata along the eastern margin of the Central Valley; his estimated magnitude of uplift is also similar to the estimates reviewed above. The estimated amounts of Late Cenozoic uplift based on tilted Late Cenozoic units are similar to those estimated from paleobotanical studies (e.g., Axelrod 1997).

The above estimates are for rock uplift. Late Quaternary erosion rates of unglaciated summit flats are low (0.002–0.015 mm/yr) (Small et al. 1997). If the Late Quaternary erosion rates are representative of Late Cenozoic rates, there has been little erosion of these summits in the Late Cenozoic, so the rock uplift estimates closely approximate surface uplift for the flat-topped summits of the Sierra Nevada crest (fig. 7). For sharp-crested summits it is probable that erosion rates have been somewhat higher. Rock-uplift estimates can also be used to evaluate the surface uplift of the bottom of canyons. Adjacent to the point of deepest Late Cenzoic incision (810 m) on the Middle Fork Feather River, the uplift of the Lovejoy Basalt is 1430–1550 m. These relationships suggest 620–740 m of Late Cenozoic surface uplift of the bottom of the most deeply incised part of the Middle Fork Feather River canyon. Similar comparison of the point of deepest incision along the Stanislaus River and uplift of the adjacent Table Mountain Latite suggests 970–1110 m of Late Cenozoic surface uplift for the bottom of the most deeply incised part of the Stanislaus River canyon. The significant surface uplift of both ridge tops and canyon bottoms indicates substantial mean surface uplift of the Sierra in the Late Cenozoic.

Unruh (1991) interpreted the initiation of uplift to correspond to regional tilting that began during the deposition of the upper Mehrten Formation at ~5 Ma. Similar tilts and ages of units along the western margin of the range suggest that uplift began at approximately the same time from the Feather River to the Kings River (Unruh 1991). Sediment accumulation rates in the Central Valley show a notable increase after deposition of the Mehrten Formation (fig. 8), consistent with the estimated ~5-Ma initiation of uplift. Huber (1981) suggested that Late Cenozoic uplift began at ~25 Ma and has progressively accelerated since then. If so, cumulative uplift (and associated rates) from 25 Ma to 5 Ma was probably minor because the inferred uplift did not measurably tilt strata along the eastern Central Valley margin (Unruh 1991) or lead to an increase of sedimentation rates in the Central Valley (fig. 8). If Late Cenozoic uplift initiated at 5 Ma, then the preferred range of uplift estimates correspond to average post-5-Ma crestal uplift rates of

0.34–0.39 mm/yr. These uplift rates are faster than post-5-Ma, east-down, vertical separation rates along the frontal fault system in the northern Sierra Nevada (fig. 2), suggesting that the crustal blocks east of the frontal faults have been uplifted relative to sea level since 5 Ma, but downdropped relative to the crest of the range. In contrast, some reaches of the frontal fault system that border the central and southern Sierra Nevada have vertical separation rates significantly greater than 0.35–0.39 mm/yr (fig. 2), suggesting subsidence relative to sea level of some crustal blocks east of the frontal faults.

Contributions of Late Cenozoic Uplift and Paleorelief to Present-Day Topography of the Sierra

Late Cenozoic uplift does not vary significantly along strike between the northern end of the range and the Kings River drainage (table 3), whereas paleorelief and maximum elevations increase systematically from the northernmost Sierra to the southern San Joaquin River drainage (figs. 3, 6). In the northern Sierra, maximum Late Cenozoic stream incision greatly exceeds paleorelief, whereas in the southern Sierra paleorelief exceeds maximum Late Cenozoic stream incision (figs. 5, 6). The difference in paleorelief between the northern and southern Sierra approximates the difference in elevations between the two regions. Another way to assess the contributions of different stages of uplift to present topography is to estimate paleoelevations by subtracting Late Cenozoic uplift estimates from present elevations (fig. 10). If the Late Quaternary erosion rates from summit flats (Small et al. 1997) are valid for the Late Cenozoic, loss of elevation from these summit flats due to erosion is 10–75 m in the last 5 Ma. On the basis of an assumption of negligible loss of elevation in the last 5 Ma, the highest paleoelevations in the Sierra north of the Yuba River drainage are <900 m, whereas peak paleoelevations increase sharply south of the Stanislaus River and are >2000 m. Paleoelevation estimates south of the San Joaquin drainage are more speculative because Late Cenozoic uplift estimates are lacking. Data of Unruh (1991) indicates that similar Late Cenozoic uplift estimates may apply as far south as the Kings River drainage, and figure 10 was constructed by extrapolating uplift estimates for the San Joaquin River drainage (Huber 1981, modified for internal deformation) as far south as the Kings River drainage. If such an extrapolation is reasonable, then the highest elevation in Sierra Nevada (Kings River drainage and north) at 5 Ma may have been in the headwaters
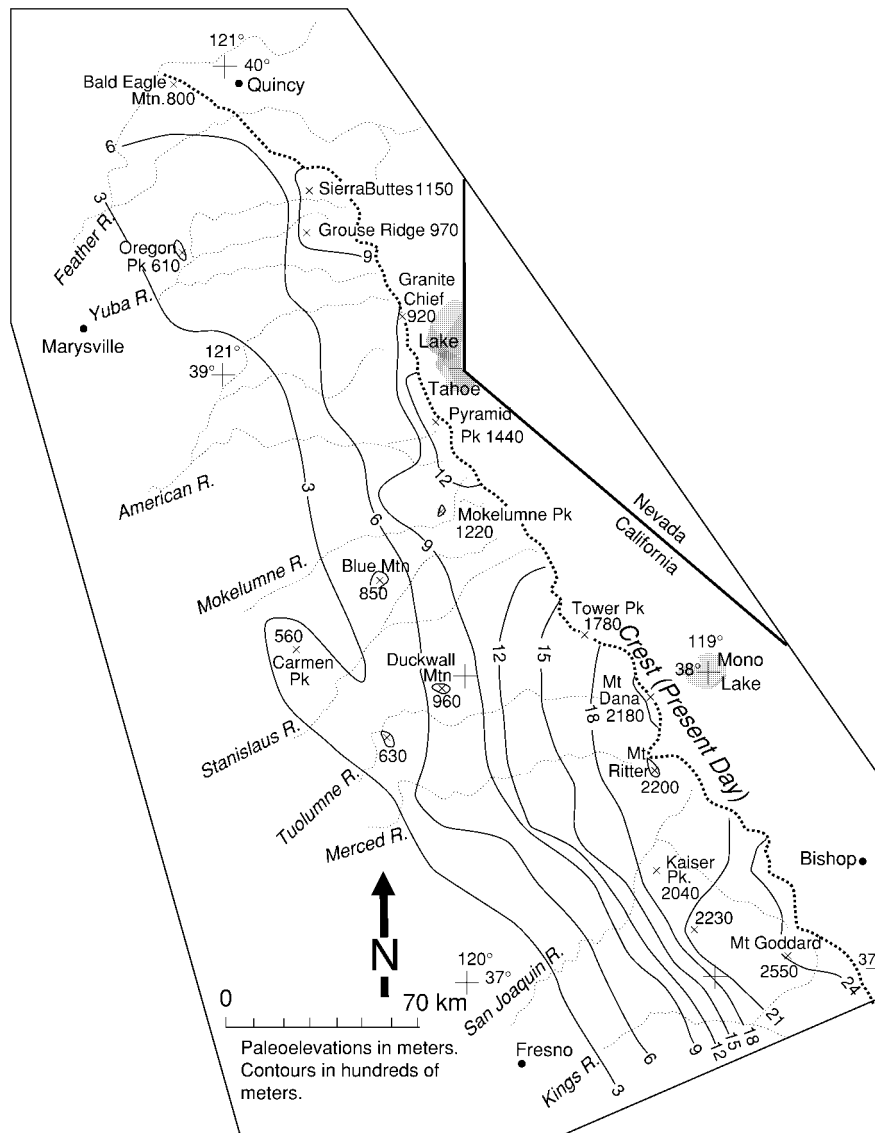
Figure 10. Generalized topography of the Sierra Nevada before Late Cenozoic uplift (~5 Ma) with smoothing of drainages as in figure 3. The map was constructed by subtracting preferred uplift estimates, scaled from crest to hingeline, from present elevations. Elevations south of the San Joaquin River drainage were calculated by extrapolating San Joaquin River drainage uplift estimates to the Kings River.

of the Kings River where paleoelevations may have exceeded 2500 m. The evaluation of paleoelevations suggests that Late Cenozoic uplift accounts for more than half of the elevation of the northern Sierra, but less than half of the elevation of the southern Sierra. Because little uplift of the Sierra Nevada appears to have occurred between 57 Ma and ~5 Ma, paleoelevations and paleorelief are probably largely relict from the earlier 99–57-Ma inferred period of uplift.

Tectonics, Uplift, and Topography

Tectonic events and associated development of relief and topography of the Sierra Nevada are summarized in the following speculative sequence of events (fig. 11): While the Cretaceous Sierra Nevada magmatic arc was still active, a major pulse of erosion and presumably rock and surface uplift began at ~99 Ma. High erosion rates persisted until ~57 Ma, ~25 Ma after the cessation of Cretaceous arc

During the last 15 Ma of arc activity, from 100 to 85 Ma, activity along transpressional fault zones causes major exhumation and erosion. Faulting migrates eastward within the arc as does magmatism. As a result, the most deeply exhumed rocks are in the west. The late Cretaceous arc, and associated shear zones, are well east of the present day Sierran block in the northern part of the range. Fault activity and erosion continues after magmatism ceases. High erosion rates persist for about 25 Ma after cessation of magmatism. Reduction of elevation and relief occur during the latter part of the 100-57 Ma period; lowering of elevation may coincide with eclogitic recrystallization of the root of the batholith following cessation of arc magmatism.

Relief and elevations have been reduced, especially in the northern part of the range. Erosion and incision rates are low in the Sierra. Laramide uplift has resulted in a regional westward slope from highlands east of the present Sierra Nevada. Large river systems flow down this slope, depositing the Eocene gold bearing gravels. The southern part of the range (and, possibly other ranges to the east) presents a topographic barrier and the Eocene streams do not cross it.

Renewed arc activity. In what is now the Sierra Nevada block, volcanic activity is confined to the northern and central parts, and covers the entire landscape in this region except for isolated basement highs. Although Basin and Range extension begins to the east, and extensional faulting encroaches progressively westward, no significant tilting or stream incision occurs in the Sierra during this time. The subducting plate margin is converted to a transform margin, thus ending arc volcanism south of the Feather River drainage.

The Walker Lane shear zone has encroached westward. Uplift begins and is associated with westward tilting of the range and east-down and dextral faulting. Uplift may be triggered by the foundering of an eclogitic root beneath the eastern Sierra. Rivers incise rapidly. In the southern Sierra, incision results in the deepening of older canyons, whereas in the northern Sierra, little relief is present before incision begins. Westward encroachment of the Frontal fault system continues, beheading many drainages in the central and northern Sierra Nevada. The greater amount of paleotopography in the southern part of the range contributes to higher elevations in that region.

Figure 11.   Tectonic diagrams of the evolution of the Sierra Nevada in the past 100 Ma

magmatism. This uplift event may have had its highest rates in the period from about 99 to 84 Ma, on the basis of sediment accumulation rates in the Great Valley Group (fig. 8). This 15-Ma period of

highest inferred erosion rates approximately coincides with the final stages of pluton emplacement of the Sierra Nevada batholith. The deformation associated with the 99–57-Ma exhumation was geo-

metrically different than the westward tilting in the Late Cenozoic. The exhumation of plutons is greatest in the western part of the range, in contrast to the Late Cenozoic tilting that has led to greater exhumation in the east, near the crest (Ague and Brimhall 1988), as reflected in the pattern of Late Cenozoic stream incision (fig. 5). Much of the exhumation of the more deeply buried western part of the batholith may have occurred before the intrusion of the youngest plutons (Dumitru 1990), and the locus of exhumation may have progressed eastward with time as did magmatism (Tobisch et al. 1995). Because the general trend of equal exhumation contours is parallel to the range axis (Ague and Brimhall 1988), differential exhumation appears to have been controlled by structures with similar strikes. These structures may be related to continued (into the Paleocene) movement on Cretaceous transpressional shear zones in the Sierra Nevada, such as the Courtright, Kern Canyon, Bench Canyon, Rosy Finch, and other shear zones (e.g., Renne et al. 1993; Tobisch et al. 1995; Tikoff and de Saint Blanquat 1997). Data presented by Tobisch et al. (1995) and Renne et al. (1993) suggest that the high-temperature movement history of these faults coincides with the 99–84-Ma period of highest Great Valley Group deposition rates (fig. 8). The eastward progression of faulting proposed by Tobisch et al. (1995) is consistent with the pattern of differential exhumation in the Sierra Nevada. Such a progression of faulting would suggest that the crest of the range migrated eastward during this period, in contrast to the westward migration of the crest during the Late Cenozoic. Loci of large amounts of exhumation may have been associated with restraining steps or bends in the dextral transpressional fault systems.

From about 80 to 45 Ma, Laramide deformation and crustal thickening took place in what is now the Great Basin, east of the Sierra Nevada (e.g., Miller et al. 1992). In the southern Sierra Nevada, the precursors to the modern canyons were established before the end of the major erosional event at 57 Ma, and their depth exceeded 1000 m locally, on the basis of paleorelief preserved in the range. Some time before the major period of erosion ended at ~57 Ma, it is likely that erosion exceeded rock uplift and resulted in a net decrease in elevation of the Sierra Nevada. The lowering of elevations in the Sierra may have been associated with the eclogitic recrystallization (and resultant density increase) of the mafic root of the Sierran batholith that occurred as a result of the decrease in geothermal gradients that accompanied the shut off of arc magmatism (Ducea and Saleeby 1996). Laram-

ide crustal thickening may have created elevated topography in what is now the Great Basin, with the development of major west-draining river systems, including those that deposited the Eocene gravels of the northern Sierra Nevada (e.g., Christiansen and Yeats 1992; Dilek and Moores 1999). These major drainages apparently crossed the Sierra Nevada only north of the present-day Stanislaus River, suggesting that the southern Sierra Nevada (and/or other ranges farther east) formed a topographic barrier at this time. Maximum elevations in the southern Sierra Nevada may have been 2500 m or higher. Thus, a significant difference in elevation and relief between the north and south Sierra Nevada may have developed by this time.

Why there is more paleorelief and higher paleoelevations in the southern part of the range is not clear. Geobarometric studies indicate that the depth of crystallization of plutons does not systematically vary significantly along strike across the regions of differing paleotopography (Ague and Brimhall 1988). However, relative to the uncertainties in pluton burial depth (up to ±3 km), the 1–2-km difference in paleoelevation and paleorelief between the north and south Sierra is probably too small to be discerned in the pattern of differential exhumation. The north to south difference in paleorelief may be a consequence of one or more of the following: (1) less surface uplift from 99–57 Ma in the northern Sierra Nevada, (2) along strike differences in the deep crust or upper mantle beneath the Sierra, and (3) earlier cessation of uplift in the northern Sierra resulting in more time to lower the elevation of that part of the range before the establishment of the Eocene drainages.

The Basin and Range began extending at about 35 Ma at the latitude of the northernmost Sierra, with extension propagating to the latitude of the southern Sierra Nevada by ~20 Ma (Dilles and Gans 1995). Westward propagation of extensional faulting also occurred, and the westernmost east-facing escarpment associated with Basin and Range or Walker Lane Belt faulting may have been as close as 35 km east of the location of the present frontal fault system at about 14 Ma (Dilles and Gans 1995). Although frontal faulting continued to encroach westward into the Sierra Nevada microplate, little tilting took place in the area that was to become the present Sierra Nevada until about 5 Ma. Volcanic arc activity began again in the Sierra Nevada at 34 Ma. From 34 to 20 Ma, this volcanism may not have been associated with a true magmatic arc, whereas after 14 Ma, eruption of the Mehrten Formation and associated deposits was apparently part of a regional magmatic arc (Christiansen and Yeats

1992). These volcanic deposits apparently covered the Sierra Nevada only north of the Tuolumne River drainage. The rejuvenation of volcanic activity does not appear to have been associated with any observable uplift or tilting of the range.

At ~5 Ma, Late Cenozoic uplift, east-down frontal faulting, and westward tilting of the Sierra Nevada began. By ~5 Ma, large-scale volcanism had ceased in much of the Sierra Nevada. Late Cenozoic uplift initiated at about the same time or a few million years after an increase in the dextral component of motion of the Sierra Nevada microplate relative to stable North America (Argus and Gordon, in press) and after a global change in relative plate motion between the Pacific and North American plates (Atwater and Stock 1998). As noted by Unruh (1991), the synchroneity of uplift along the length of the range indicates that initiation of uplift was not related to migration of the Mendocino triple junction. Uplift may have been driven by the foundering of an eclogitic root beneath the eastern Sierra that resulted in lithospheric buoyancy relative to surrounding regions (Ducea and Saleeby 1996). Data from xenoliths in Late Cenozoic volcanic rocks suggest that an eclogitic root to the Sierra Nevada existed until ~8–12 Ma, after which it foundered (Ducea and Saleeby 1998). Manley et al. (2000) suggested that the foundering or delamination event may have occurred as recently as 3.5 Ma, on the basis of a suggested tie between delamination and a newly dated pulse of potassic volcanism in the southern Sierra Nevada. Although these studies presented strong evidence for delamination, it is not clear whether this delamination event can explain roughly synchronous initiation of uplift and frontal faulting along the entire Sierra Nevada because the studies were based on volcanic rocks from the southern Sierra. However, heat flow is similar along the length of the eastern Sierra (Lachenbruch and Sass 1977), consistent with a delamination event having occurred beneath the entire range.

Small and Anderson (1995) suggested climatic, rather than tectonic, triggering at 3 Ma for initiation of Sierran incision and tilting, but this appears to be about 2 m.yr. younger than the initiation of Late Cenozoic tilting and incision as estimated in this article and by Unruh (1991). The approximate synchroneity of the initiation of tilting, stream incision, faulting along the frontal fault system, the change in Sierra Nevada microplate relative motion, and inferred delamination beneath the Sierra suggests that a tectonic transition probably triggered Late Cenozoic uplift. Uplift and tilting may have been enhanced by an isostatic response to Sierran erosion and Central Valley deposition (Small and Anderson 1995).

As Late Cenozoic uplift progressed, westward encroachment of the Walker Lane Belt continued, resulting in the beheading of drainages and westward jumps of the crest of the Sierra Nevada. Rapid Late Cenozoic stream incision in the Sierra eroded deep canyons through Cenozoic deposits and into the basement beneath these deposits. Late Cenozoic extensional deformation in the Basin and Range province may have resulted in the lowering of mean elevation in that region (e.g., Wolfe et al. 1997) in contrast to the mean surface uplift in the Sierra Nevada.

Significant paleorelief exists in the Sierra, particularly south of the Stanislaus River drainage. Sierran topography is thus a superposition of topography generated by the ongoing Late Cenozoic uplift with a significant contribution from relict topography apparently related to an uplift event that took place in a much different tectonic setting and ended at least 50 m.yr. before the present one began.

REFERENCES CITED

Ague, J. J., and Brimhall, G. H. 1988. Magmatic arc asymmetry and distribution of anomalous plutonic belts in the batholiths of California: effects of assimilation, crustal thickness, and depth of crystallization. Geol. Soc. Am. Bull. 100:912–927.

Argus, D. F., and Gordon, R. G. 1991. Current Sierra Nevada–North America motion from very long baseline interferometry: implications for the kinematics of the western United States. Geology 19:1085–1088.

———. In press. Present tectonic motion across the Coast Ranges and San Andreas fault system in central California. Geol. Soc. Am. Bull.

Atwater, T., and Stock, J. 1998. Pacific-North America plate tectonics of the Neogene southwestern United States: an update. Int. Geol. Rev. 40:375–402.

Axelrod, D. I. 1962. Post-Pliocene uplift of the Sierra Nevada, California. Geol. Soc. Am. Bull. 76:183–198.

———. 1997. Paleoelevation estimated from Tertiary floras. Int. Geol. Rev. 39:1124–1133.

Axelrod, D. I., and Ting, W. S. 1960. Late Pliocene floras east of the Sierra Nevada. Univ. Calif. Pub. Geol. Sci. 39:1–117.

Bachman, S. B. 1978. Pliocene-Pleistocene break-up of the Sierra Nevada-White-Inyo Mountains block and the formation of Owens Valley. Geology 6:461–463.

Bacon, C. R.; Giovanetti, D. M.; Duffield, W. A.; and Dalrymple, G. B. 1979. New constraints on the age of the Coso Formation. Geol. Soc. Am. Abstr. Program 11:67.

Bailey, R. A. 1989. Geologic map of the Long Valley Caldera, Mono-Inyo Craters volcanic chain, and vicinity, eastern California. U.S. Geol. Surv. Misc. Investig. Ser. Map I-1933, scale 1 : 62,500.

Bartow, J. A. 1979. Age control for the latest movements on the Melones fault zone in the Sierra foothills belt from K-Ar dates for Late Tertiary intrusions. U.S. Geol. Surv. Open File Rep. 79-582, 12 p.

———. 1985. Map and cross sections showing Tertiary stratigraphy and structure of the northern San Joaquin Valley, California. U.S. Geol. Surv. Misc. Field Studies Map MF-1761, scale 1 : 250,000.

———. 1990. The Late Cenozoic evolution of the San Joaquin Valley, California: U.S. Geol. Surv. Prof. Pap. 1501, 40 p.

Bateman, P. C., and Wahrhaftig, C. 1966. Geology of the Sierra Nevada. In Bailey, E. H., ed. Geology of northern California. Calif. Div. Mines Geol. Bull. 190:107–172.

Beanland, S., and Clark, M. M. 1995. The Owens Valley fault zone, eastern California, and surface rupture associated with the 1872 earthquake. U.S. Geol. Surv. Bull. 1982.

Berggren, W. A.; Kent, D. V.; Swisher, C. C., III; and Aubry, M.-P. 1995. A revised Cenozoic geochronology and chronostratigraphy. In Berggren, W. A.; Kent, D. V.; Aubry, M.-P.; and Hardenbol, J., eds. Geochronology time scales and global stratigraphic correlation. SEPM Spec. Pub. 54:129–212.

Chen, J. H., and Moore, J. G. 1982. Uranium-lead isotopic ages from the Sierra Nevada batholith. J. Geophys. Res. 87:4761–4784.

Christensen, M. N. 1966. Late crustal movements in the Sierra Nevada of California. Geol. Soc. Am. Bull. 77: 163–182.

Christiansen, R. L., and Yeats, R. S. 1992. Post-Laramide geology of the U.S. Cordilleran region. In Burchfiel, B. C.; Lipman, P. W.; and Zoback, M. L., eds. The Cordilleran orogen: conterminous (Geology of North America. Vol. G-3). Boulder, Colo., Geol. Soc. Am. p. 261–403.

Clark, M. M.; Harms, K. K.; Lienkaemper, J. J.; Harwood, D. S.; Lajoie, K. R.; Matti, J. C.; Perkins, J. A.; et al. 1984. Preliminary slip rate table and map of Late Qua-

ternary faults of California. U.S. Geol. Surv. Open File Rep. 84-106.

Curtis, G. H. 1954. Mode of origin of the pyroclastic debris in the Mehrten Formation of the Sierra Nevada. Univ. Calif. Dept. Geol. Sci. Bull. 29:453–502.

Dalrymple, G. B. 1964. Cenozoic chronology of the Sierra Nevada, California. Univ. Calif. Pub. Geol. Sci. 47. 41 p.

Dilek, Y., and Moores, E. M. 1999. A Tibetan model for the early Tertiary western United States. J. Geol. Soc. Lond. 156:929–941.

Dilles, J. H., and Gans, P. B. 1995. The chronology of Cenozoic volcanism and deformation in the Yerington area, western Basin and Range and Walker Lane. Geol. Soc. Am. Bull. 107:474–486.

Dixon, T. H.; Miller, M.; Farina, F.; Wang, H.; and Johnson, D. 2000. Present-day motion of the Sierra Nevada block and some tectonic implications for the Basin and Range province, North American Cordillera. Tectonics 19:1–24.

Ducea, M., and Saleeby, J. B. 1996. Buoyancy sources for a large, unrooted mountain range, the Sierra Nevada, California: evidence from xenolith thermobarometry. J. Geophys. Res. 101:8229–8244.

———. 1998. A case for delamination of the deep batholithic crust beneath the Sierra Nevada. Int. Geol. Rev. 40:78–93.

Dumitru, T. A. 1990. Subnormal Cenozoic geothermal gradients in the extinct Sierra Nevada magmatic arc: consequences of Laramide and post-Laramide shallow-angle subduction. J. Geophys. Res. 95:4925–4941.

Durrell, C. 1966. Tertiary and Quaternary geology of the northern Sierra Nevada. In Bailey, E. H., ed. Geology of northern California. Calif. Div. Mines Geol. Bull. 190:185–197.

Evernden, J. F., and Kistler, R. W. 1970. Chronology of emplacement of Mesozoic batholith complexes in California and western Nevada. U.S. Geol. Surv. Prof. Pap. 623, 28 p.

Gradstein, F. M.; Agterberg, F. P.; Ogg, J. G.; Hardenbol, J.; VanVeen, P.; Thierry, J.; and Huang, Z. 1995. A Triassic, Jurassic, and Cretaceous time scale. In Berggren, W. A.; Kent, D. V.; Aubry, M.-P.; and Hardenbol, J., eds. Geochronology time scales and global stratigraphic correlation. SEPM Spec. Pub. 54:95–126.

Grant, T. A.; McCleary, J. R.; and Blum, R. L. 1977. Correlation and dating of geomorphic and bedding surfaces on the east side of the San Joaquin Valley using dip. In Singer, M. J., ed. Soil development, geomorphology and Cenozoic history of the northeastern San Joaquin Valley and adjacent areas, California. Guidebook for joint field session (ASA, SSSA, GSA). Davis, University of California Press, p. 312–318.

House, M. A.; Wernicke, B. P.; and Farley, K. A. 1998. Dating topography of the Sierra Nevada, California, using apatite (U-Th)/He ages. Nature 396:66–69.

House, M. A.; Wernicke, B. P.; Farley, K. A.; and Dumitru, T. A. 1997. Cenozoic thermal evolution of the central Sierra Nevada, from (U-Th)/He thermochronometry. Earth Planet. Sci. Lett. 151:167–179.

Huber, N. K. 1981. Amount and timing of Late Cenozoic uplift and tilt of the central Sierra Nevada, California—evidence from the upper San Joaquin river basin. U.S. Geol. Surv. Prof. Pap. 1197, 28 p.

———. 1990. The Late Cenozoic evolution of the Tuolumne River, central Sierra Nevada, California. Geol. Soc. Am. Bull. 102:102–115.

Hyne, N. J.; Chelminski, P.; Court, J. E.; Gorsline, D. S.; and Goldman, C. R. 1972. Quaternary history of Lake Tahoe, California-Nevada. Geol. Soc. Am. Bull. 83: 1435–1448.

Ingersoll, R. V. 1979. Evolution of the Late Cretaceous forearc basin, northern and central California. Geol. Soc. Am. Bull. 90:813–826.

Jones, L. M., and Dollar, R. S. 1986. Evidence of basin-and-range extensional tectonics in the Sierra Nevada: the Durrwood Meadows swarm, Tulare County, California (1983–1984). Bull. Seismol. Soc. Am. 76: 439–461.

Lachenbruch, A. H., and Sass, J. H. 1977. Heat flow in the United States and the thermal regime of the crust. *In* Heacock, J. G., ed. The Earth's crust, its nature and physical properties. Am. Geophys. Union Geophys. Monogr. 20:626–675.

Lindgren, W. 1911. The Tertiary gravels of the Sierra Nevada of California. U.S. Geol. Surv. Prof. Pap. 73, 226 p.

Manley, C. R.; Glazner, A. F.; and Farmer, G. L. 2000. Timing of volcanism in the Sierra Nevada of California: Evidence for Pliocene delamination of the batholithic root? Geology 28:811–814.

Matthes, F. E. 1930. The Devils Postpile and its strange setting. Sierra Club Bull. 15:1–8.

Miller, D. M.; Nilsen, T. H.; and Bilodeau, W. L. 1992. Late Cretaceous to Early Eocene geologic evolution of the U.S. Cordillera. *In* Burchfiel, B. C.; Lipman, P. W.; and Zoback, M. L. eds. The Cordilleran orogen: conterminous (Geology of North America, Vol. G-3). Boulder, Colo., Geol. Soc. Am., p. 205–260.

Moore, J. G., and Dodge, F. C. W. 1980. Late Cenozoic volcanic rocks of the southern Sierra Nevada, California. I. Geology and petrology. Geol. Soc. Am. Bull. 91:515–518.

Moxon, I. 1988. Sequence stratigraphy of the Great Valley in the context of convergent margin tectonics. *In* Graham, S. A., ed. Studies of the geology of the San Joaquin basin. Pac. Sec. SEPM 60:3–28.

Muntean, T. W.; Cashman, P.; and Trexler, J. 1999. Tectonic evolution of the Neogene Gardnerville sedimentary basin, western Nevada. Geol. Soc. Am. Abstr. Program 31:A81.

Noble, D. C.; Slemmons, D. B.; Korringa, M. K.; Dickinson, W. R.; Al-Rawi, Y.; and McKee, E. 1974. Eureka Valley Tuff, east-central California and adjacent Nevada. Geology 2:139–142.

Pakiser, L. C.; Kane, M. F.; and Jackson, W. H. 1964. Structural geology and volcanism of the Owens Valley region, California: a geophysical study. U.S. Geol. Surv. Prof. Pap. 438, 68 p.

Phillips, F. M.; McIntosh, W. C.; and Dunbar, N. W. 2000.

Extensional collapse of the Owens Valley during the Late Pliocene. Geol. Soc. Am. Abstr. Program 32:A-507.

Ransome, F. L. 1898. Some lava flows on the western slope of the Sierra Nevada, California. U.S. Geol. Surv. Bull. 89. 71 p.

Renne, P. R.; Tobisch, O. T.; and Saleeby, J. B. 1993. Thermochronologic record of pluton emplacement, deformation, and exhumation at Courtright shear zone, central Sierra Nevada, California. Geology 21: 331–334.

Riebe, C. S.; Kirchner, J. W.; Granger, D. E.; and Finkel, R. C. 2000. Erosional equilibrium and disequilibrium in the Sierra Nevada, inferred from cosmogenic 26Al and 10Be in alluvial sediment. Geology 28:803–806.

Roberts, C. T. 1985. Cenozoic evolution of the northwestern Honey Lake basin, Lassen County, California. Colo. School Mines Q., Vol. 80, 73 p.

Saleeby, J. B., and Sharp, W. D. 1980. Chronology of the structural and petrologic development of the southwest Sierra Nevada foothills, California. Geol. Soc. Am. Bull. 91:1416–1535.

Saucedo, G. J., and Wagner, D. L. 1992. Geologic map of the Chico quadrangle. Calif. Div. Mines Geol. Reg. Geol. Map Ser. Map 7A, scale 1 : 250,000.

Sharp, W. D.; Turrin, B. D.; Renne, P. R.; and Lanphere, M. A. 1996. The ^{40}Ar/^{39}Ar and K/Ar dating of lavas from the Hilo 1-km core hole, Hawaii Scientific Drilling Project. J. Geophys. Res. 101:11,607–11,616.

Slemmons, D. B. 1966. Cenozoic volcanism of the central Sierra Nevada, California. *In* Bailey, E. H., ed. Geology of northern California. Calif. Div. Mines Geol. Bull. 190:199–208.

Slemmons, D. B.; Van Wormer, D.; Bell, E. J.; and Silberman, M. L. 1979. Recent crustal movements in the Sierra Nevada-Walker Lane region of California-Nevada. I. Rate and style of deformation. Tectonophysics 52:561–570.

Small, E. E., and Anderson, R. S. 1995. Geomorphically driven Late Cenozoic rock uplift in the Sierra Nevada, California. Science 270:277–280.

———. 1998. Pleistocene relief production in Laramide mountain ranges, western United States. Geology 26: 123–126.

Small, E. E.; Anderson, R. S.; Repka, J. L.; and Finkel, R. 1997. Erosion rates of alpine bedrock summit surfaces deduced from in situ 10Be and 26Al. Earth Planet. Sci. Lett. 150:413–425.

Stern, T.W.; Bateman, P. C.; Morgan, B. A.; Newell, M. F.; and Peck, D. L. 1981. Isotopic U-Pb ages of zircon from granitoids of the central Sierra Nevada, California. U.S. Geol. Surv. Prof. Pap. 1185, 17 p.

Tikoff, B., and de Saint Blanquat, M. 1997. Transpressional shearing and strike-slip partitioning in the Late Cretaceous Sierra Nevada magmatic arc, California. Tectonics 16:442–459.

Tobisch, O. T.; Saleeby, J. B.; Renne, P. R.; McNulty, B.; and Tong, W. 1995. Variations in deformation fields during the development of a large-volume magmatic

arc, central Sierra Nevada, California. Geol. Soc. Am. Bull. 107:148–166.

Trexler, J. H., Jr.; Cashman, P. H.; and Henry, C. D. 1999. The Verdi basin: a syntectonic Neogene basin in western Nevada. Geol. Soc. Am. Abstr. Program 31:A103.

Unruh, J. R. 1991. The uplift of the Sierra Nevada and implications for Late Cenozoic epeirogeny in the western Cordillera. Geol. Soc. Am. Bull. 103:1395–1404.

Wagner, D. L.; Jennings, C. W.; Bedrossian, T. L.; and Bortugno, E. J. 1981. Geologic map of the Sacramento Quadrangle. Calif. Div. Mines Geol. Reg. Geol. Map Ser. Map 1A, scale 1 : 250,000.

Wahrhaftig, C. W. 1965. Stepped topography of the southern Sierra Nevada, California. Geol. Soc. Am. Bull. 76:1165–1189.

Wakabayashi, J.; Page, W. D.; Renne, P. R.; Sharp, W. D.; and Becker, T. A. 1994. Plio-Pleistocene volcanic rocks and incision of the North Fork Feather River, California: Tectonic implications. *In* Lanphere, M. A.; Dalrymple, G. B.; and Turrin, B. D., eds. Eighth International Conference of Geochronology Cosmo-chronology, and Isotope Geology. Abstracts. U.S. Geol. Surv. Circ. 1107:345.

Wakabayashi, J., and Sawyer, T. L. 2000. Neotectonics of the Sierra Nevada and the Sierra Nevada-Basin and Range Transition, California, with field trip stop descriptions for the northeastern Sierra Nevada. *In* Brooks, E. R., and Dida, L. T., eds. Field guide to the geology and tectonics of the northern Sierra Nevada. Calif. Div. Mines Geol. Spec. Pub. 122:173–212.

Wentworth, C. M., and Zoback, M. D. 1989. The style of later Cenozoic deformation at the eastern front of the California Coast Ranges. Tectonics 8:237–246.

Whitney, J. D. 1880. The auriferous gravels of the Sierra Nevada of California. Harv. Coll. Mus. Comp. Zool. Mem. Vol. 6, 569 p.

Wolf, R. A.; Farley, K. A.; and Kass, D. M. 1998. Modeling of the temperature sensitivity of the apatite (U-Th)/He thermochronometer. Chem. Geol. 148:105–114.

Wolfe, J. A.; Schorn, H. E.; Forest, C. E.; and Molnar, P. 1997. Paleobotanical evidence for high altitudes in Nevada during the Miocene. Science 276:1672–1675.

Yeend, W. H. 1974. Gold bearing gravel of the ancestral Yuba River, California. U.S. Geol. Surv. Prof. Pap. 722.